The Impact of Large-Scale Macroalgae Cultivation and Harvesting Strategies on the Marine Carbon Dioxide Removal Efficacy and Marine Biogeochemistry

Prima Anugerahanti[1], Julien Palmiéri[2], Chelsey A. Baker[2], Ekaterina Popova[2], and Andrew Yool[2]

[1]National Oceanography Centre, Joseph Proudman Building, 6 Brownlow Street, Liverpool L3 5DA, UK
[2]National Oceanography Centre, European Way, Southampton SO14 3ZH, UK

Correspondence: Prima Anugerahanti (prianu@noc.ac.uk)

Abstract. The large-scale cultivation of macroalgae has been proposed as a marine carbon dioxide removal (mCDR) strategy, yet its efficiency and consequences for ocean biogeochemistry remain uncertain. Using a new macroalgae aquaculture module within an ocean biogeochemistry model, NEMO-MEDUSA, we investigate carbon removal potential and biogeochemical feedbacks under hypothetical global-scale macroalgae cultivation with varying harvest strategies, loss rates, and iron availability. Overall cultivation enhances air–sea CO_2 uptake by 11.0 Pg C yr^{-1}, but only ∼27% of macroalgal production results in additional CO_2 uptake. Furthermore, phytoplankton and zooplankton biomass is suppressed by almost 50% and is geographically displaced by significant surface nutrient changes. Sinking of harvested biomass increases oxygen demand during remineralisation, leading to widespread oxygen depletion and the emergence of suboxic conditions at the seafloor in deposition regions. When macroalgal growth is not supplemented with iron micronutrient, its production declines sharply (-74%), revealing a significant limitation for large-scale feasibility. Collectively, our results reveal that large-scale macroalgal cultivation offers low mCDR potential, that it is both spatially extensive and locally intensive, and its unintended biogeochemical consequences can be substantial. Our findings highlight the urgent need to assess nutrient constraints and ecological trade-offs before considering this method as a viable large-scale mCDR strategy.

1 Introduction

Since the adoption of the Paris Agreement in 2015 and the publication of the IPCC Sixth Assessment Report, carbon dioxide removal (CDR) strategies have become increasingly recognised as essential to meet the global climate targets (IPCC, 2022). Among marine-based approaches, the cultivation of macroalgae (seaweed) has been suggested as a promising CDR strategy, due to its efficient uptake of dissolved inorganic carbon (DIC), facilitated by its high carbon-to-nitrogen (C:N) ratio (Duarte et al., 2021; Froehlich et al., 2019; Sheppard et al., 2023). In addition to this potential carbon sequestration, macroalgae can confer multiple ecological co-benefits depending on their deployment, including providing habitat for invertebrates and

fish, mitigation of eutrophication, and shoreline protection (Barrett et al., 2022; Corrigan et al., 2022; Duarte et al., 2017). Furthermore, macroalgae may act as a substitute for carbon-intensive industrial products, such as food, animal feed, and biofuels, and contribute indirectly to emission reductions (DeAngelo et al., 2022). These attributes have garnered interest in scaling macroalgae aquaculture offshore, which may increase its potential contribution to marine CDR (N'Yeurt et al., 2012; Froehlich et al., 2019).

Relative to terrestrial agriculture, macroalgae aquaculture, which predominantly occurs in coastal zones, requires minimal fertiliser aside from iron (Fe) supplementation (Yamamoto et al., 2017) and has lower associated emissions (Koesling et al., 2021). Current applications are predominantly toward food production (Naylor et al., 2021) and producing biochar for agricultural use (Roberts et al., 2015). However, most of these uses return the carbon fixed by macroalgae to the atmosphere on timescales too short to be climate-relevant, so does not provide a long-term reservoir for carbon sequestration. In natural systems, a substantial fraction of macroalgal NPP is released as particulate and dissolved organic carbon (POC and DOC), as demonstrated by experimental and field-based estimates (Kennedy and Blain, 2025; Chen et al., 2020), which may either be consumed and/or respired or exported to the deep ocean or seafloor sediments where long-term storage may occur over climate-relevant timescales (Krause-Jensen and Duarte, 2016). In contrast, aquaculture practices commonly involve harvesting the biomass at the end of the growing season or after it reaches a target biomass (Arzeno-Soltero et al., 2023). While cultivated macroalgae release DOC and POC during growth, the removal of standing biomass during harvest limits the macroalgae-sequestered carbon, than can be exported to the deep ocean, and therefore limiting the contribution to climate-relevant carbon sequestration (Hurd et al., 2023). To ensure durable storage of macroalgae carbon, active sinking of harvested biomass to the deep ocean has been proposed as a potential strategy (Froehlich et al., 2019; Alevizos and Barillé, 2023), despite studies suggesting that replacing carbon intensive products, such as fertiliser and fuels, with macroalgae-based products would have greater potential for reducing atmospheric greenhouse gas than by sinking macroalgae for sequestration (Roque et al., 2019; Bullen et al., 2024).

There are two critical challenges in evaluating the efficacy of all mCDR methods: 1. quantifying additional atmospheric CO_2 uptake by the ocean relative to an established baseline, and 2. robustly estimating durability of additional carbon storage (Boyd and Vivian, 2019). Macroalgae photosynthesis induces a local DIC deficit in seawater, shifting air–sea CO_2 equilibrium, which promotes CO_2 uptake from the atmosphere (Hurd et al., 2023). The rate of equilibration depends on environmental conditions: weeks to months in coastal areas, several months to a year in open-ocean settings, and more than a year in high-latitude or ice-covered regions (Jones et al., 2014; Bach et al., 2021). If DIC-deficient water is rapidly subducted before atmospheric equilibration occurs, CO_2 removal may not occur (Hurd et al., 2023; Bach et al., 2021).

When assessing the CDR potential of macroalgae cultivation, the minimum criterion is that, in utilising the resources and space of natural ecosystems, their activity sequesters more atmospheric CO_2 than the background natural system. In an observational study, Jiang et al. (2013) found that phytoplankton can be as effective at driving ocean uptake of CO_2 as cultivated macroalgae. Since both macroalgae and phytoplankton rely on the same limiting resources, such as light, nitrogen (N), and phosphorus (P), intensive macroalgae aquaculture may reduce phytoplankton biomass through competitive exclusion (Boyd et al., 2022), potentially diminishing primary production of macroalgae and phytoplankton leading to an increase in outgassing

(Berger et al., 2023). On larger spatial scales, macroalgae nutrient uptake could alter regional nutrient fluxes. For example, in the Southern Ocean, large-scale cultivation may induce "nutrient trapping" (Wu et al., 2023), a phenomenon where nutrient removal and transport to the deep ocean by macroalgae limits downstream phytoplankton production in the low latitudes because less nutrients are transported out of the Southern Ocean, as previously simulated in ocean Fe fertilisation experiments (Tagliabue et al., 2023).

Prior to large-scale implementation of macroalgae cultivation, it is essential to estimate the potential CDR efficiency and assess its impact on marine biogeochemistry. Global ocean biogeochemical (OBGC) models provide a suitable scale for undertaking these assessments. Previous studies have estimated the potential of large-scale macroalgae CDR under different assumptions, such as different nutrient scenarios (Arzeno-Soltero et al., 2023; Berger et al., 2023; Wu et al., 2023). Large-scale simulations of macroalgae cultivation consistently show that nutrient limitations Arzeno-Soltero et al. (2023) and competition with phytoplankton Wu et al. (2023); Berger et al. (2023) can reduce macroalgae production, air-sea CO_2 flux, and therefore CDR efficiency. Moreover, large-scale deployment could negatively impact ocean ecosystems; such as lowering phytoplankton productivity, expanding oxygen minimum zones (Wu et al., 2023; Berger et al., 2023), and can lead to net decreases in carbon sequestration (Bach et al., 2021).

To optimise large-scale offshore macroalgae CDR, it is important to assess constraints beyond nutrient limitation, such as considering other cultivation protocols, micronutrient fertlisation and limitation, biomass sinking, and remineralisation pathways as these affect CDR efficiency and may impede natural carbon cycling. We address three key questions in this study:

1. To what extent can macroalgae cultivation and harvesting lead to additional oceanic CO_2 uptake?
2. How does large-scale macroalgae cultivation modify nutrient and light availability, and what are the resulting biogeochemical responses of phytoplankton and the biological pump?
3. What are the consequences of remineralisation-induced deoxygenation at depth when we sink harvested macroalgae biomass?

We investigate these questions using global simulations of an OBGC model that includes macroalgae in a new marine aquaculture submodel, simulated under the 'near-present-day' period under observational forcing. This framework allows us to explore a range of cultivation and harvesting scenarios to assess mCDR efficacy and evaluate its wider impacts on marine ecosystems and processes.

Our study extends previous global assessments of macroalgae cultivation (e.g. Wu et al., 2023; Arzeno-Soltero et al., 2023; Berger et al., 2023; Wu et al., 2025; Berger et al., 2025) by incorporating a suite of cultivation protocol experiments that explore the effects of harvest threshold, non-harvest loss, biomass extraction, nutrient supplementation, and limitation. This framework allows us to quantify how different modelling assumptions and protocols affect ocean biogeochemistry, including air-sea CO_2 flux, nutrient distribution, seafloor oxygen, and phytoplankton NPP, providing a more comprehensive view of large-scale macroalgae cultivation in the global ocean.

2 Method

2.1 Ocean Model

Our study uses a macroalgae model embedded within a coupled physical-biogeochemical ocean model. Ocean physics is represented by the Nucleus for European Modelling of the Ocean framework (NEMO; Madec (2016)). NEMO is composed of an ocean general circulation model coupled to a separate sea-ice model, the Sea Ice modelling Integrated Initiative (SI3; Group (2023)). The NEMO domain used here (the extended ORCA1 grid; eORCA1) is at a horizontal resolution of approximately 1-degree, and uses a tripolar model grid and incorporates an equatorial band of enhanced resolution. Vertical space in NEMO is resolved into 75 z-levels that range in thickness from approximately 1 m at the surface to approximately more than 200 m at abyssal depths.

Ocean biogeochemistry is represented by the Model of Ecosystem Dynamics, nutrient Utilisation, Sequestration and Acidification (MEDUSA; Yool et al. (2013)). MEDUSA is a dual size-class "intermediate complexity" ecosystem/biogeochemistry model that resolves nutrients and two size classes of phytoplankton, zooplankton, and detritus (NPZD) components. The smaller size class includes non-diatom phytoplankton, microzooplankton and small particles of slow-sinking detritus, while the larger size class includes diatoms, mesozooplankton and large particles of fast-sinking detritus (the latter modelled implicitly). The biogeochemical cycles of N, Fe, C, silicon, oxygen, and alkalinity are represented, coupled in both fixed and dynamic stoichiometric relationships.

Air-sea CO_2 flux in NEMO-MEDUSA is calculated prognostically using standard equations for the partition of dissolved inorganic carbon (DIC) into dissolved CO_2 and carbonic acid, bicarbonate, and carbonate ions. Partitioning is a function of local temperature, salinity, DIC, and total alkalinity, and uses the MOCSY-2.0 carbonate chemistry routines (Orr and Epitalon, 2015). The exchange of CO_2 with the atmosphere is then calculated from the dissolved CO_2 fraction, atmospheric CO_2, temperature, salinity, and surface winds, following the gas transfer parameterisation of Wanninkhof (2014). Because gas transfer is finite and wind speed dependent, the rate at which surface ocean pCO_2 anomalies equilibrate with the atmosphere is limited, introducing a natural lag between biological carbon drawdown and atmospheric CO_2 uptake. A full description of MEDUSA can be found in Yool et al. (2013), with the current version evaluated in Yool et al. (2021).

The ocean model is forced at its surface boundary using a climatologically-adjusted version of the ERA-5 atmospheric reanalysis (Hersbach et al., 2020). Ocean physical fields and the biogeochemical fields of oxygen and nutrients (N and silicon) are initialised using the World Ocean Atlas 2023 (Reagan et al., 2024). As simulations are initialised from a time-point prior to the reference period of the GLODAP climatology (Lauvset et al., 2016), dissolved inorganic carbon (DIC) and alkalinity fields are initialised from prior simulations of the model (in the UKESM1 framework; Yool et al. (2021)) to minimise bias in the CO_2 air-sea flux due to model equilibration. For other plankton tracers we use uniform nominal values. Riverine nutrient inputs are not included in this configuration, so nutrient supply is limited to oceanic initial conditions and internal cycling.

This initial state is then simulated for two cycles of the forcing period between 1976 to 2024 (2×49 years $= 98$ years). This is done so that surface biogeochemical properties reach quasi-equilibrium, minimising the drift during the experimental period when macroalgae are introduced (see subsection 2.2). Note that, since DIC has a strong secular signal during the 1976–

2024 period caused by rising atmospheric pCO_2, its concentration is reset to the 1976 UKESM1 state at the beginning of each forcing cycle, and the rising atmospheric pCO_2 is still simulated during the simulation until the end of the cycle. The temperature increase within this simulated period is relatively small compared to late 21st-century warming used in other CDR studies (e.g. in Palmiéri and Yool (2024)) and therefore show limited effects on the macroalgae and other biogeochemical tracers.

2.2 Macroalgae Module

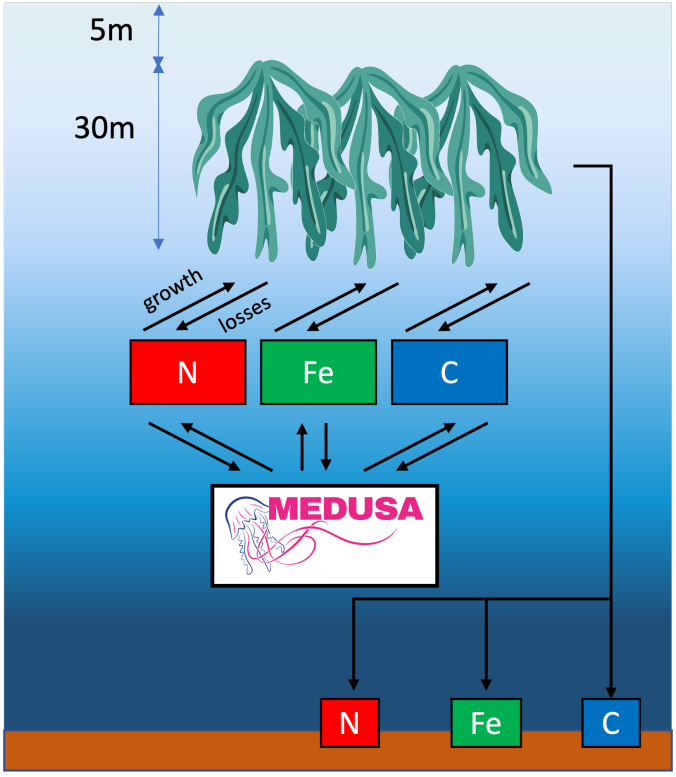

Figure 1. Schematic diagram of the macroalgae model. Macroalgae is grown 5m below the surface, consuming C, N, and Fe. In the model, we limit the macroalgae growth to 30m. Seaweed cultivation includes non-harvest loss and harvesting, where the latter is directly sunk to the seafloor, contributing to seafloor DIN, DIC, DFe, and Oxygen.

mCDR by macroalgae is simulated by adding a new aquaculture module to MEDUSA. This module effectively represents macroalgae as being cultivated on a fabricated floating structure that is anchored and immobile (Ross et al., 2022; Wu et al., 2023). As such, macroalgae is located on the ocean model's grid but it is not advected by ocean currents, although it interacts with MEDUSA's advected passive tracers. We assume that macroalgae cultivation started from the last 20 years of the control run (2004-2023), starting from a small initial biomass of 0.01 mmol N m^{-3}. This initial value is consistent with other biological

tracers in MEDUSA and serves as an "inoculation", after which biomass grows in response to temperature, light and nutrient limitation.

Fundamentally, the macroalgae growth and loss processes are similar to those of phytoplankton with the key differences subsequently outlined. Unlike MEDUSA's phytoplankton, modelled macroalgae biomass is static within the model grid and has a restricted vertical extent, by default from approximately 5 to 30 m in the water column (10 model levels) following previous modelling studies (Wu et al., 2023, 2025) and offshore cultivation experiment (Zollmann et al., 2023; Tullberg et al., 2022). This depth range is intended to represent large-scale offshore cultivation and differs from nearshore farming practices, where shallower deployments are common (e.g. Choi et al. (2025); Sato et al. (2023); Hwang et al. (2018)). In an initial simulation, we found negligible differences between cultivating macroalgae between 1-30m and 5-30m (results not shown). Functionally, macroalgae growth is loosely based on that of MEDUSA's phytoplankton, with separate chlorophyll (Chl) and N biomass, and with its rate governed by temperature and the availability of light and dissolved inorganic nitrogen (DIN) and iron (DFe). No external nutrient inputs or pulsed fertilisation are applied. As a result macroalgae compete directly with phytoplankton for the same nutrient resources. Fig. 1 presents a schematic of the macroalgae model and its relationships with MEDUSA's dissolved tracers.

In terms of loss processes, while the simulated macroalgae incur non-harvest losses, they are assumed not to be explicitly grazed by zooplankton. However, their cultivation involves active harvesting, the precise mechanism and fate of which forms part of the experimental design described below.

Following the work of Arzeno-Soltero et al. (2023), we use multiple species in our macroalgae module with: two cold water species (*Macrocystis* and *Saccharina*) and two warm water species (*Sargassum* and *Euchema*). These taxa span a board range of thermal niches and cultivation context: cold water species usually occupies high latitude nutrient-rich upwelling system, commonly found in the North Atlantic aquaculture industry (Veenhof et al., 2024), while warm water species are predominantly cultivated in tropical and subtropical regions (Hayashi et al., 2017; Magcanta-Mortos et al., 2025). All four are represented in identical functional from, with a number of shared parameters, but each species has different values for certain key parameters. These include optimal temperature range (between T^1_{opt} and T^2_{opt}), half-saturation constant for DIN uptake (k_{DIN}), and C:N ratio ($\Theta_{\text{C:N}}$) adopted from Arzeno-Soltero et al. (2023). Although these taxa differ in their real-world cultivation methods and physiological traits, they are represented using a common idealised cultivation framework to isolate first-order biogeochemical effects at large spatial scales. We acknowledge that growth rates, carbon content, and other physiological traits vary considerably across and within taxa in reality (Sato et al., 2025), but our choice rather reflects a functional representation designed to capture first-order biogeochemical effects at global scale. Our analysis therefore focuses on the sensitivity of large-scale biogeochemical responses to macroalgal cultivation.

Macroalgae growth is limited by temperature (T_L), light (L_L), and nutrient (N_L), and its losses comprises of non-harvest loss $Loss_{\text{noharv}}$ and harvesting loss $Loss_{\text{harv}}$. Therefore the change in each macroalgae type, M_n is calculated by:

$$\frac{dM_n}{dt} = \text{Growth} - Loss_{\text{noharv}} - Loss_{\text{harv}} \tag{1}$$

Table 1. Parameter table for different macroalgae species. The different macroalgae parameters are based on Arzeno-Soltero et al. (2023) (Supplementary material). C:N ratio is based on the initial cell quota of different macroalgae species from the same study. We apply a common set of physiological parameters across macroalgal taxa in order to focus on first-order biogeochemical responses rather than species-specific physiological variability.

Parameter	**Symbol**	**Units**	*Saccharina*	*Sargassum*	*Eucheuma*	*Macrocystis*
DIN half-saturation uptake constant	k_{DIN}	mmol N m^{-3}	2.00	2.95	5.60	10.13
Optimum Temperature 1	$T_{1,opt}$	°C	10.0	20.5	22.5	13.0
Optimum Temperature 2	$T_{2,opt}$	°C	15.0	25.5	27.5	18.0
Biomass C:N ratio	$\Theta_{\text{C:N}}$	mol C (mol N)$^{-1}$	26.8	34.3	34.3	26.8
Maximum growth rate	μ_m	day^{-1}	0.2 (Zhang et al., 2016; Arzeno-Soltero et al., 2023)			
Chl-a specific initial slope of P-I curve	$\hat{\alpha_m}$		15 (Enríquez et al., 1996)			
DFe half-saturation uptake constant	k_{DFe}	mmol Fe m^{-3}	1.5×10^{-3} (Paine et al., 2023)			
Biomass Fe:N ratio	$\Theta_{\text{Fe:N}}$	mol N (mol Fe)$^{-1}$	5.08×10^{-3} (Sharma et al., 2018)			
Non-harvest loss	$m2_{max}$	day^{-1}	0.025 (Arzeno-Soltero et al., 2023)			
Adjusted coefficient lower T limit	β_1		0.03 (Arzeno-Soltero et al., 2023)			
Adjusted coefficient upper T limit	β_2		0.1 (Arzeno-Soltero et al., 2023)			
Fraction of macroalgae that are harvested	$m1_{max}$	day^{-1}	0.9			
Target harvesting threshold	TH	mmol N m^{-2}	400 (Bak et al., 2018; Wang et al., 2020)			
Carbon content of dry macroalgae	C_{DW}		0.3 (Chung et al., 2011)			
Wet weight : Dry Weight	WW:DW		9.33 (Van Der Molen et al., 2018)			

The temperature limitation term is similar to a Gaussian probability curve with flat peak, adopted from Arzeno-Soltero et al. (2023):

$$T_L = \exp\left(\beta_1 (T - T_{1,opt})^2\right), T < T_{1,opt} \tag{2}$$

$$T_L = \exp\left(\beta_2 (T - T_{2,opt})^2\right), T > T_{2,opt} \tag{3}$$

$$T_L = 1, T = T_{opt} \tag{4}$$

Where T_{opt} is a 5°C optimal temperature range for each macroalgae group. β_1 and β_2 are adjusted near the lower (β_1) and upper temperature limits (β_2) to reach zero, respectively. The temperature limitation function acts as a smooth growth filter rather than a binary on-off switch. As such, growth declines gradually as temperature departs from the optimal range for each represented taxon, ensuring more realistic transitions across latitude and season.

Light limitation is formulated in the same way as in phytoplankton:

$$L_L = \frac{\mu T_L \hat{\alpha_m} I}{\left(\mu T_L\right)^2 + \hat{\alpha_m}^2 I^2)^{0.5}} \tag{5}$$

Where I is the irradiance and $\hat{\alpha}$ is the initial slope of photosynthesis-irradiance curve, so that macroalgae with a high chlorophyll content have an elevated response to irradiance.

Macroalgae compete with phytoplankton to obtain nutrients (n), and nutrient uptake (n_{up}) is formulated using Michaelis-Menten kinetics:

$$n_{up} = \frac{n}{k_m + n} \tag{6}$$

Unlike the default formula for phytoplankton, in the macroalgae default simulation, we assume that Fe is supplemented ($Fe_{up} = 1$) and only DIN is the limiting nutrient. However, we allow multiple nutrient limitation, by using the Liebig's law of minimum, described below (N_L):

$$N_L = \min(DIN_{up}, Fe_{up}) \tag{7}$$

In addition to harvesting, simulated macroalgae experience non-harvest losses, which represents biomass losses outside deliberate harvesting, such as physical erosion, aging, fragmentation, and implicit grazing processes. Non-harvesting loss are transferred directly to the slow detrital pool, where they are remineralised according to the standard MEDUSA slow sinking detritus formulation. As a result, processes such as direct DOC release during production are implicitly subsumed within the detrital pathway rather than treated explicitly:

$$Loss_{\text{noharv}} = m2_{max} M_n \tag{8}$$

Where $m2_{max}$ is the rate of mortality.

For harvesting, once total integrated macroalgae biomass at a grid point has reached the target harvesting threshold (TW), it is harvested over the course of a single simulated day, using a linear loss term and parameter $m1_{max}$. Otherwise, the macroalgae continues to grow.

$$Loss_{\text{harv}} = m1_{max} M_n \tag{9}$$

In the default case, harvested macroalgae biomass is assumed to be baled-up and immediately sunk to the seafloor in the same water column, so that the associated carbon biomass is durably stored and isolated from the surface ocean and atmosphere. This process is formulated similarly to that of fast-sinking organic detritus in MEDUSA (see Section 2.3.10 of Yool et al. (2013)), but with a different remineralisation length-scale, and without the influence of any biomineral ballasting. The value of the length-scale is set to considerably deeper than the seafloor (40 km) to represent this active baling and deposition that aims to ensure that the harvested biomass reaches the seafloor does not undergo substantial decay. The organic material reaching the seafloor in this way is added to MEDUSA's existing benthic reservoirs and is remineralised from these in the same manner as material arriving via the natural biological pump (i.e. slow remineralisation to DIN, DIC and DFe with the associated consumption of oxygen). This approach avoids cultivated macroalgae biomass undergoing remineralisation in the upper water column and increases the efficiency with which fixed CO_2 is stored in the ocean (and removed from exchange with the atmosphere).

Note that MEDUSA resolves biological respiration and remineralisation for both phytoplankton and macroalgae at every depth level and timestep. Air-sea CO_2 flux is therefore driven by the net change in surface DIC after all biological produc-

tion, community respiration, grazing, and remineralisation processes operate, rather than by NPP alone. The net ecosystem production (NEP) signal is thus an emergent property of the model's coupled biological and chemical state.

After initialisation and a spin-up period (see subsection 2.1), we run the control model (NEMO-MEDUSA only) using ERA-5 forcing from 1976 until 2024. We assume that macroalgae cultivation started from the last 20 years of the control run (2004-2023). We will focus on quantifying CO_2 sequestration, biomass harvested, and assessing how harvesting strategy would affect ocean biogeochemistry including nutrient cycles (N and Fe), phytoplankton net primary production (NPP) and plankton biomass, carbonate chemistry (air-sea CO_2 flux), seafloor oxygen, and carbon pool distributions. The results shown in this manuscript are the average from 2015-2024.

2.3 Experimental Design

To assess the biogeochemical impacts of large-scale macroalgae cultivation, we compare a baseline MEDUSA simulation with one incorporating dynamic macroalgae growth (MEDUSA + Macroalgae). Building on this framework, we conduct four sensitivity experiments to explore key intervention strategies and test modelling uncertainties:

1. varying the biomass threshold for harvesting and sinking
2. increasing non-harvest loss
3. extracting harvested biomass from the ocean system entirely rather than sinking it
4. applying Fe limitation.

These experiments and shorthands are summarised in Table 2.

Table 2. Experiment summary table. Macroalgae experiments are initialised from the Control simulation in 2004 and simulated for 20 years.

Experiment	**Simulation description**	**Run period**
Control	NEMO-MEDUSA	1976–2023
Default (Harvest 400)	+ Macroalgae, harvest at 400 mmol N m^{-2}, Fe fertilised	2004–2023
Harvest 200	+ Macroalgae, harvest at 200 mmol N m^{-2}, Fe fertilised	2004–2023
Harvest 800	+ Macroalgae, harvest at 800 mmol N m^{-2}, Fe fertilised	2004–2023
High Loss	+ Macroalgae, non harvesting loss = 0.05 day^{-1}, Fe fertilised	2004–2023
Extraction	+ Macroalgae, no biomass sinking, Fe fertilised	2004–2023
Fe limitation	+ Macroalgae, with Fe limitation	2004–2023

In all experiments we define the target biomass as the sum of local integrated macroalgae biomass in mmol N m^{-2}. The default target biomass is 400 mmol N m^{-2} (500 g dry weight (DW) m^{-2}), resulting in two harvests a year on average based on studies by Bak et al. (2018); Wang et al. (2020), although warmer macroalgae species can be harvested up to 12 times a year (Valderrama et al., 2013). To assess the sensitivity of target biomass in harvesting, we vary the weight to 200 and 800

mmol N m^{-2}. Macroalgae are not harvested until they reach these target biomasses, so will continue to grow until they do (and will continue to experience non-harvest losses). Harvesting involves decreasing the biomass of macroalgae by 90% during the harvest day. Since Fe is one of the limiting nutrients for macroalgae, we prescribe Fe:N ratio of 5.1×10^{-3} and half saturation constant of 1.5×10^{-3} based on laboratory studies (Sharma et al., 2018; Paine et al., 2023). However, in the default simulation (as well as all other experiments except for Fe limitation), we assume that macroalgae are only limited by DIN. This corresponds to an assumption that Fe is supplemented, following established farming practices Yamamoto et al. (2017), and that it is at non-limiting (replete) concentrations. When macroalgae is being remineralised, the added Fe will also be released. Additionally, parameter values used in these equations are described in Table 1.

To determine whether CDR is efficient within a certain region, we use two different CDR efficiency metrics; efficiency calculated using macroalgae NPP ($CDR_{eff\ NPP}$) and harvested macroalgae biomass ($CDR_{eff\ Harv}$). $CDR_{eff\ NPP}$ can be calculated as the proportion between macroalgae NPP and the additional air-sea CO_2 flux within each grid cell (CDR flux) (Berger et al., 2023) :

$$CDR_{eff\ NPP} = \frac{CO_2\ flux_{macroalgae} - CO_2\ flux_{control}}{\text{Macroalgae NPP}} \times 100\% \tag{10}$$

If annual average macroalgal NPP associated carbon is equivalent to the annual average of additional atmospheric CO_2 uptake within a grid cell then the CDR efficiency would be 100%, as it is assumed that the macroalgae-induced DIC deficit within the grid cell has driven the CO_2 uptake. The calculation of $CDR_{eff\ NPP}$ is therefore a net measure, incorporating macroalgal production, phytoplankton feedback, and air-sea carbon equilibration collectively (Berger et al., 2023). It should be noted that we use annual average macroalgae NPP, to account for macroalgae seasonality, whereas the modelling study by Berger et al., 2023 uses prescribed maximal macroalgal NPP.

To calculate how much carbon is assumed to be durably stored, we calculate CDR efficiency using the proportion between harvested macroalgae biomass and the CDR flux (Wu et al., 2025; Ocean Visions and Monterey Bay Aquarium Research Institute, 2022):

$$CDR_{eff\ Harv} = \frac{CO_2\ flux_{macroalgae} - CO_2\ flux_{control}}{\text{Macroalgae Harvest}} \times 100\% \tag{11}$$

3 Results

3.1 Seaweed Production and Harvesting

In the default simulation, macroalgae occupies 51.7 $\times 10^6$ km^2, accounting for approximately 14.35% of the global ocean surface. Macroalgae were primarily distributed across nitrogen-rich surface waters and major upwelling zones, including the Equatorial Pacific, North Pacific, North Atlantic, Southern Ocean, and coastal regions such as Chile, Argentina and Namibia (Fig. 2a). The average annual macroalgae NPP of 111.1 gC $m^{-2}yr^{-1}$ (40.34 Pg C yr^{-1}) was similar in magnitude to the average phytoplankton NPP from the control run (47.7 Pg C yr^{-1}). The most dominant macroalgae species are *Saccharina* and *Sargassum* in high and low latitudes, respectively (see Supplementary Fig. S1), with the former contributing the most to macroalgae

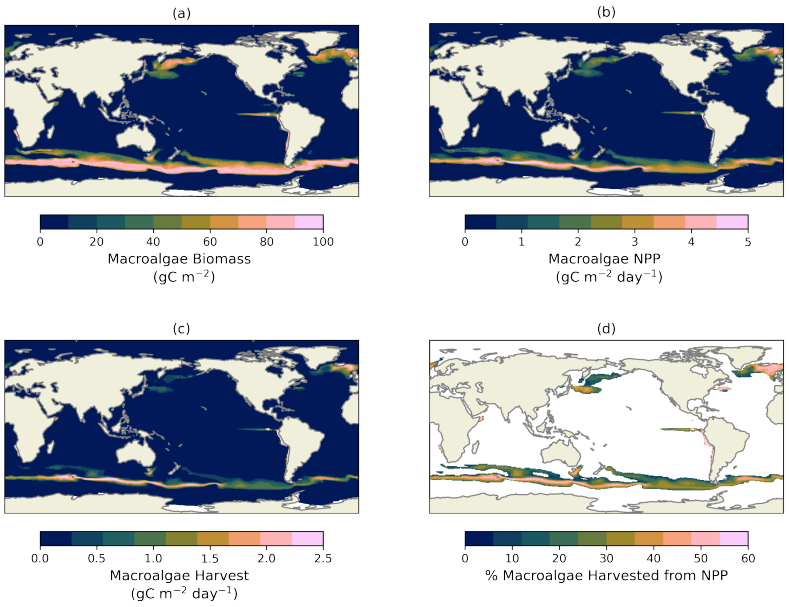

Figure 2. Macroalgae Biomass (a), NPP (b), harvest (c), and percentage of how much NPP are harvested (d) from the default experiment averaged between 2015-2024.

NPP (36.11 Pg C yr^{-1}). The annual harvest yield that is sunk to the deep ocean reached 135.59 tonne Dry Weight (tDW) km^{-2} (12.5 Pg C yr^{-1}), 31.1% of the macroalgae NPP, with a high proportion harvested in the North Atlantic, Southern Ocean, and along the coast of Chile (Fig. 2b, c, d, and 3). The spatial patterns of macroalgae, NPP, and nutrients shown here are emergent outcomes of open-ocean biogeochemical conditions within a coarse-resolution global model, and should be interpreted as indicating potential cultivation areas and not as plausible regions for macroalgae farms. Many regions identified as productive for macroalgae would present extreme technological, logistical, and societal challenges.

Different cultivation protocols and model assumptions affect macroalgae outcomes. Varying the harvesting threshold changes NPP magnitude while preserving the general spatial pattern (Supplementary Fig. S2 & S3). Harvest 800 led to less harvested biomass (-8.7%), higher area of coverage (+6.28%), and higher macroalgae NPP (+49%). Harvest 200 decreases macroalgae coverage (-5.43%), reduced total macroalgae NPP (-30%), and modestly raised the harvested biomass (+13%) due to more frequent harvest (see Fig.3). This resulted in a higher harvest efficiency (i.e., harvested biomass as a fraction of macroalgae NPP, see Supplementary Fig. S3b) compared to the default simulation (Harvest 400). Other protocols also affected macroalgae production, Fig. 3. Extraction shows slight decreases of macroalgae NPP and area (by -1.37%). Introducing Fe limitation (i.e. stopping Fe supplementation), dramatically suppressed macroalgae growth and harvest was almost entirely eliminated

(–99.2%), and the cultivated area shrank by 47.95%. Macroalgae NPP also declined by 72.8%, especially in regions where Fe concentration is low, such as the Equatorial and North Pacific (see Supplementary Fig. S2f). Higher non-harvesting loss also significantly reduced macroalgae area (44.6%), NPP and harvest.

3.2 mCDR Efficiency and CO_2 Flux

Under default simulation conditions assuming no Fe limitation, global-scale macroalgae cultivation enhanced net air–sea CO_2 flux by approximately 11.0 Pg C yr^{-1} (equivalent to 40.3 Pg CO_2 yr^{-1}; Fig. 3), while without macroalgae, CO_2 flux is only 1.4 Pg C yr^{-1}, indicating a substantial contribution to marine carbon dioxide removal (mCDR). The increase in CO_2 flux under the default simulation is sufficient to limit warming to 2° (between 0.7-3.6 Pg C yr^{-1} (DeAngelo et al., 2021; IPCC, 2022)). Although 31.1% of primary production is being harvested and sunk, the $CDR_{eff\ NPP}$ (the proportion of additional CO_2 flux to macroalgae NPP) was only 27.3% but $CDR_{eff\ Harv}$ was 87.9%. $CDR_{eff\ NPP}$ also varied regionally. High-efficiency zones ($CDR_{eff\ NPP}$ >50%) were simulated along the Southern Ocean, while low-efficiency areas (<10%) emerged in the central Equatorial Pacific, off the western coast of North Japan, and offshore South Africa (Fig. 4c). Areas off southern coast of Chile, exhibited net outgassing due to surface DIC accumulation (Fig. 4b). Since additional CO_2 flux often occurs outside harvesting area (Fig. 2c and Fig. 4b), we do not show efficiency maps for $CDR_{eff\ Harv}$.

The mCDR efficiency is sensitive to cultivation protocol. Harvest 200 slightly decreased the CO_2 flux, improved the $CDR_{eff\ NPP}$ to 38.4% (Macroalgae NPP of 27.95 Pg C yr^{-1}, CDR flux of 10.73 Pg C yr^{-1}), but slightly lowers $CDR_{eff\ Harv}$ to 86.1%, due to lower CDR flux. Whereas Harvest 800 reduced the CDR flux to 9.6 Pg C yr^{-1} and lowered $CDR_{eff\ NPP}$ to 16.0%, but slight increases $CDR_{eff\ Harv}$ to 89.4%. In all threshold scenarios, the Equatorial Pacific consistently showed the lowest $CDR_{eff\ NPP}$, whilst modest improvements occurred in the Southern Ocean under the low-threshold scenario (Supplementary Fig. S4b).

Further amendments to the cultivation strategies and modelling assumptions also influenced mCDR outcomes, Fig. 3. The High Loss experiment increases macroalgae NPP to 60.18 Pg C yr^{-1} because of the regenerated nutrients from non-harvesting loss, but reduced global CO_2 flux into the ocean to 7.3 Pg C yr^{-1}, because there are less macroalgae harvested and sunk, which reduces $CDR_{eff\ NPP}$ to 16.0%, but slightly increases $CDR_{eff\ Harv}$ to 88.4%. Extraction increased the global CO_2 flux by 0.13 Pg C yr^{-1}, because of less remineralisation in shallow waters, which induced CO_2 flux. This protocol also has the highest $CDR_{eff\ Harv}$ of 91.7% due to higher CDR flux. Simulating realistic Fe limitation constraints on macroalgae growth causes outgassing by contributing 0.2 Pg C yr^{-1} to the atmosphere, indicating that scaled-up macroalgae cultivation without Fe fertilisation is not an effective mCDR technique (negative CDR efficiency, -1.6%).

3.3 Impact of Macroalgae Cultivation on Ocean Biogeochemistry

Macroalgae cultivation had significant effects on surface nutrient concentrations and oxygen levels, primarily in areas of cultivation and harvesting, summarised in Table 3. In the default simulation, surface DIN declined by 53.1%. This decline was co-located with high macroalgae productivity. Because of the assumption of Fe supplementation, surface DFe increases by 90.26% from non-harvesting loss. Furthermore, to grow macroalgae ubiquitously in the default run, on average 1.4 Pg Fe yr^{-1}

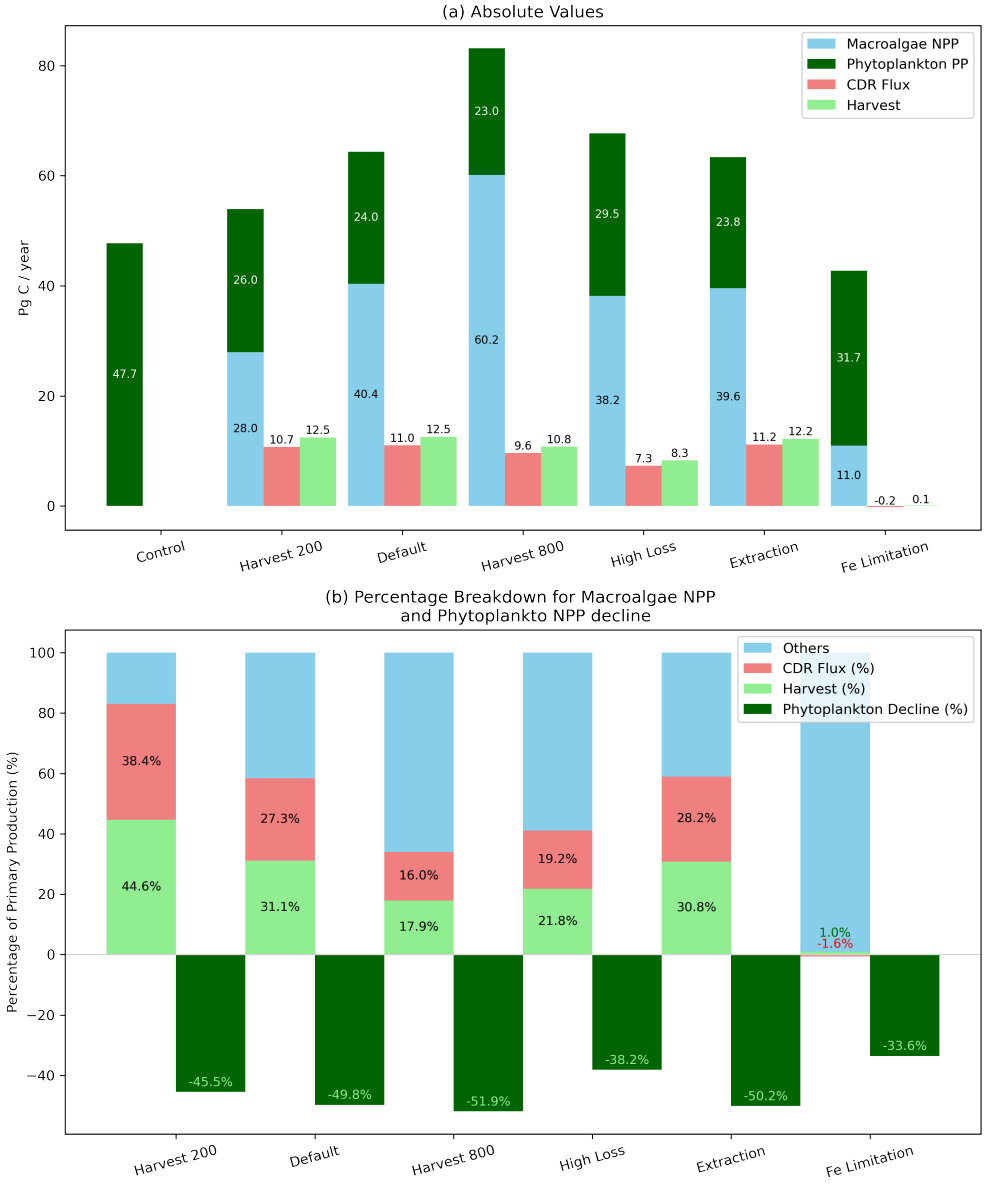

Figure 3. Global macroalgae cultivation and its influence on air–sea carbon flux across all experiments averaged between 2015-2024. (a) Absolute values of macroalgae primary production, phytoplankton primary production, the resulting enhancement in air–sea CO_2 exchange (CDR flux), and harvest in Pg C yr^{-1}. (b) CDR efficiency and harvest expressed as a proportion of macroalgae NPP ($CDR_{eff\,NPP}$). Dark green bar shows the decline of phytoplankton net primary production.

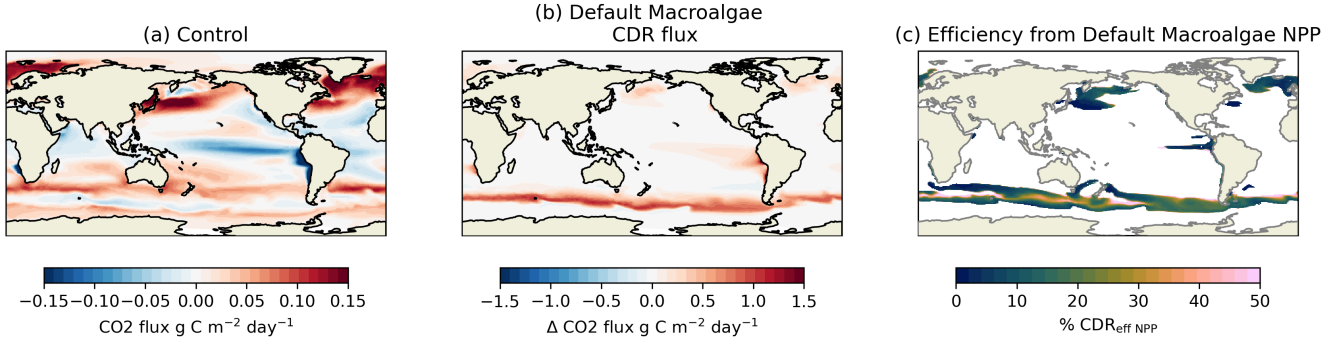

Figure 4. CO_2 flux for (a) the control and (b) the difference between control and default macroalgae simulations. We also calculate the proportion of additional CO_2 flux and macroalgae NPP, expressed as $CDR_{\text{eff Harv}}$.

was added to the ocean. The increased DFe occurs in areas occupied by macroalgae. DIN and DFe accumulation was also found near the seafloor at deposition sites, reflecting remineralisation of sunken biomass. Due to high Fe:N ratio of macroalgae, the increase in seafloor DFe can reach up to 3x the control simulation.

Table 3. Summary of absolute concentrations and percentage changes across macroalgae cultivation protocols, relative to the control simulation, for DIN and Fe at the surface and seafloor, Oxygen at the seafloor, as well as integrated phytoplankton NPP, surface phytoplankton, and zooplankton biomass.

	control	Harvest 200	Default	Harvest 800	High Loss	Extraction	Fe limitation
Surface DIN (mmol m^{-3})	6.19	3.08	2.90	2.85	3.56	2.89	9.11
Δ (%)		-50.3	-53.1	-53.9	-42.5	-53.3	+47.2
Surface DFe (mmol m^{-3})	0.60×10^{-3}	1.10×10^{-3}	1.14×10^{-3}	1.22×10^{-3}	0.85×10^{-3}	1.13×10^{-3}	0.42×10^{-3}
Δ (%)		+83.6	+90.3	+102.8	+41.1	+89.1	-30.7
Seafloor DIN (mmol m^{-3})	30.31	31.01	30.96	30.86	30.76	29.81	30.17
Δ (%)		+2.3	+2.1	+1.8	+1.5	-1.7	-0.5
Seafloor DFe (mmol m^{-3})	0.55×10^{-3}	1.61×10^{-3}	1.59×10^{-3}	1.42×10^{-3}	0.56×10^{-3}	0.55×10^{-3}	0.55×10^{-3}
Δ (%)		+195.1	+191.7	+159.5	+3.0	+1.3	+1.6
Seafloor oxygen (mmol m^{-3})	205.5	162.6	163.7	168.8	176.6	205.8	205.1
Δ (%)		-20.9	-20.3	-17.9	-14.1	+0.2	-0.2
Phytoplankton (mmol m^{-3})	0.37	0.22	0.20	0.19	0.24	0.20	0.27
Δ (%)		-40.7	-45.4	-48.1	-35.8	-46.0	-26.1
Zooplankton (mmol m^{-3})	0.26	0.13	0.14	0.16	0.17	0.13	0.19
Δ (%)		-49.6	-47.2	-36.8	-34.5	-48.1	-27.8
Phytoplankton NPP (Pg C yr^{-1})	47.7	26.0	24.0	23.0	29.5	23.8	31.7
Δ (%)		-45.5	-49.8	-51.9	-38.2	-50.2	-33.6

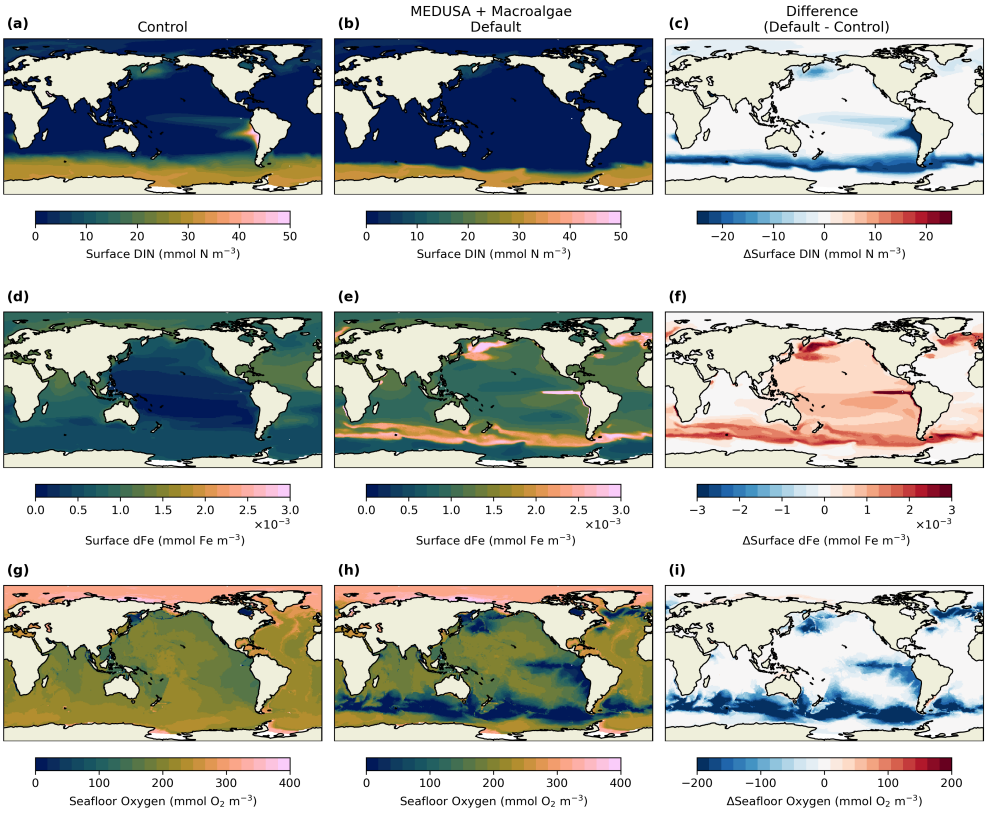

Figure 5. Changes in nutrients distribution in the surface between control and the default macroalgae simulation. a, d, and g show DIN, DFe, and seafloor oxygen from the control simulation, respectively, while from the default simulations are shown in b, e, and h. The difference between the two simulations are shown in c, f, and i

Altering the harvest threshold had a significant effect on surface nutrients (Table 3 and Supplementary Fig. S5a-h). Harvest 200 shows slightly weaker DIN drawdown (–50.3%), while Harvest 800 showed a slightly stronger DIN drawdown (–53.9%). These experiments also produce higher and lower surface DFe compared to the control simulation (83.56% and 102.84% more DFe for Harvest 200 and Harvest 800, respectively). Among the alternative cultivation protocols, higher non-harvesting loss rate leads to less DIN decline (-42.5%) and lower DFe increase (41.05%). In contrast, the Extraction experiment removed the benthic DIN enrichment entirely, and shows a slight benthic DFe increase, while having similar surface impacts to the default run. For the Fe limited experiment, the surface DIN and DFe increases and decreases by 47.2% and -30.7%, respectively. At the seafloor, the DIN concentration declines by 0.48% because of the lack of harvest but DFe increases by 1.64% due to high Fe:N ratio.

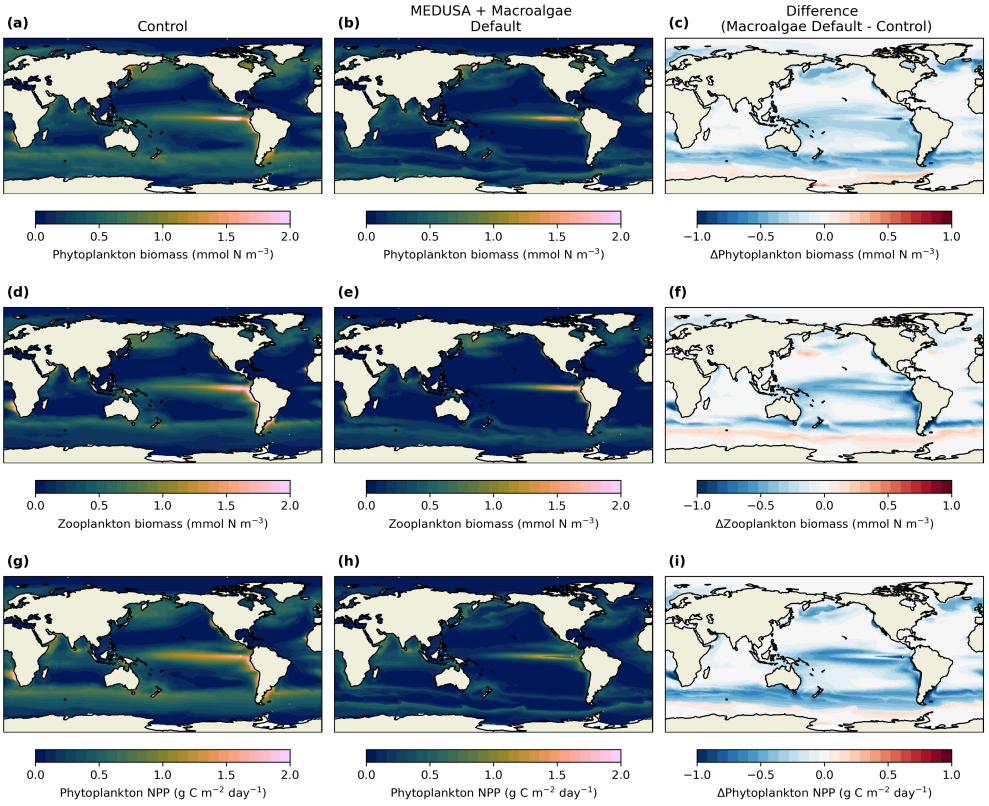

Figure 6. Plankton biomass and phytoplankton NPP and how it changes after macroalgae cultivation. The top, middle, and bottom rows show phytoplankton biomass, zooplankton biomass, and phytoplankton NPP. Control simulations are shown in a, d, and g, while b, e, and h shows the default macroalgae simulation. The difference between the two simulations are shown in c,f, and i.

Oxygen concentrations were affected by both macroalgae growth and biomass disposal. At the seafloor, oxygen losses reached 20.3% on average globally, but can reach 70% decline in the harvesting and deposition areas (see Fig. 2c). These areas can also become suboxic (Fig. 5k), which covers 7.9% of the seafloor, compared to 0.5% in the control simulation.

Impact on oxygen concentration is closely linked with harvesting threshold (Table 3 and Supplementary Fig. S5o-u, S6). Harvest 200 led to greater seafloor oxygen loss. Whereas Harvest 800 reduced oxygen depletion at the seafloor due to less deposition. Similarly, High Loss shows lower oxygen loss in the deep ocean, as less macroalgae is harvested (see Fig. 3). In contrast, the Extraction experiment eliminated benthic oxygen loss. The inclusion of Fe limitation also shows very low benthic oxygen less compared to other experiments owing to suppressed harvest and sinking (Supplementary Fig. S6f,g)

Large-scale macroalgae cultivation substantially altered surface nutrient availability and light conditions, leading to pronounced changes in the phytoplankton NPP. Note that these changes reflect competition for nutrients and light as represented in the model and provide an indicative estimate of the potential biogeochemical response, rather than a detailed prediction of

realised ecosystem behaviour. In the default simulation, phytoplankton NPP fell by 49.78% (–24.81 Pg C yr^{-1}), accompanied by declines of in phytoplankton biomass (45.40%) and zooplankton biomass (47.16%), with the largest reductions in nutrient-rich and upwelling regions (Fig. 6 b,e,h). There are also areas where both phytoplankton and zooplankton concentrations are increasing, such as the polar Southern Ocean (Fig. 6 d,e,f), which may occur due to the increase in DFe concentration (Fig. 5d-f). Adjusting harvesting threshold modified the severity but not the direction of these changes (Supplementary Fig. 7c,d,j,k) : Harvest 200 slightly alleviated phytoplankton biomass and NPP losses but intensified zooplankton declines, while Harvest 800 worsened phytoplankton and NPP reductions but not as much zooplankton decline as the default run.

Other modelling considerations, such as imposing higher non-harvest loss would reduce less phytoplankton biomass, NPP, and zooplankton biomass. Extraction had little effect on plankton dynamics compared to the default, suggesting that surface processes dominate short-term responses. Imposing Fe limitation sharply constrained macroalgal growth and partly restored surface nutrients, especially DIN, yet phytoplankton and zooplankton showed net decline (Table 3), although regions such as the Indian, Atlantic, and parts of North Pacific did exhibit increased phytoplankton and zooplankton concentrations (Supplementary Fig. S7). These results underscore that ecosystem-wide impacts persist even when macroalgae productivity is minimal.

4 Discussion

Our study extends previous large-scale macroalgal cultivation modelling by focusing on cultivation protocols, such as harvesting and extracting biomass, physiological constraints, and biogeochemical feedbacks using the NEMO–MEDUSA ocean biogeochemistry model. This approach allowed us to assess not only the theoretical mCDR potential of large-scale macroalgae cultivation, but also the ecological trade-offs associated with different deployment strategies and assumptions.

Our default simulation is broadly consistent with previous observations and models. Simulated macroalgae NPP (111.1 gC m^{-2} yr^{-1}) falls within the observed global range of 91-522 gC m^{-2} yr^{-1} (Hurd et al., 2014; Duarte et al., 2017; Paine et al., 2021. The simulated harvesting yield of 135.6 tDW km^{-2}, is slightly smaller than previous modelling study (Wu et al., 2023), yet remains within the observational range (Peteiro et al., 2014). Macroalgae biomass hotspots align with previously reported patterns from models (e.g. Arzeno-Soltero et al., 2023; Wu et al., 2023) and the estimated suitable ocean area for macroalgae cultivation, (51.7×10^6 km^2 of the ocean) agrees with previous estimates using N:P ratios and Earth system models (Froehlich et al., 2019; Wu et al., 2023). These agreements show that our simulation captures the key first-order biogeochemical drivers relevant to large-scale macroalgae cultivation.

From the default simulation, global macroalgae cultivation has the potential to increase CO_2 uptake by 11.0 Pg C yr^{-1} exceeding the amount required to align with 2°C climate pathway (0.7-3.6 Pg C yr^{-1} by mid-century DeAngelo et al., 2022; IPCC, 2022). This magnitude is higher than the earlier global cultivation study of Wu et al. (2023) (3.63 Pg C yr^{-1}), which may be due to no phosphate limitation and Fe supplementation in our simulation. Relative to macroalgal NPP the increase in CO_2 uptake remains modest ($\sim$27%, see Fig. 3), and is lower than a modelling cultivation study within EEZs (58%; Berger et al., 2023). It is important to note that the 27% CDR efficiency already accounts for the displacement of phytoplankton productivity. $CDR_{eff\ NPP}$ measures the fraction of macroalgal NPP that results in additional CO2 uptake by the ocean, relative to a control

simulation without macroalgae (Equation 10, following Berger et al., 2023). The 50% suppression of phytoplankton NPP reported in Section 3.3 is therefore not an additional loss to be subtracted from the 27% figure, it is already embedded within it. In other words, macroalgae cultivation under the default scenario replaces roughly half of the natural biological pump while delivering only 27% additional CDR, highlighting the modest net climate benefit relative to the scale of ecosystem disruption. This reflects the strong nutrient constraints on biotic mCDR.

Although up to 87.9% of the CO_2 uptake in our simulations is associated with harvested and sunk biomass, only 31% of macroalgal production is actually harvested, indicating that most fixed carbon is lost than durably stored. While our idealised experiments allow macroalgae cultivation over large oceanic areas, such configuration should be viewed as upper-bound scenarios. When cultivation is restricted to shelf-sea area (depth $<$ 200m, supplementary figures S8), simulated CO_2 uptake is reduced to 0.81 Pg C yr^{-1} using default simulation condition, higher than that in previous EEZ study (0.21 Pg C yr^{-1}, Berger et al. (2023)). This also suggests that constraining the spatial extent of cultivation affects the magnitude, rather than direction of biogeochemical response. As with other biotic CDR approaches, the net removal ultimately depends on both biogeochemical constraints and equilibration timescales governing air–sea CO_2 exchange.

4.1 Biogeochemical Impacts

The enhanced CO_2 uptake in the default scenario was accompanied by major biogeochemical side-effects. Macroalgae cultivation reduced global phytoplankton NPP and zooplankton biomass by almost half the control model, which is caused by DIN depletion in surface waters. This decline exceeded 50%, consistent with nutrient robbing seen in previous modelling studies (Aldridge et al., 2021; Boyd et al., 2022; Wu et al., 2023). However it is also important to note that the macroalgae submodule includes only a simple loss term and does not explicitly resolve grazing or other higher trophic food-web feedbacks (e.g. in Wu et al., 2023, 2025 zooplankton grazing is explicitly represented). Additionally, MEDUSA only represents two phytoplankton functional types, which do not fully capture the diversity of nutrient acquisition strategies and ecological responses present in natural systems. As a result, the simulated reduction in phytoplankton NPP and zooplankton biomass reported here may represent an overestimation, because explicit herbivory on macroalgae could recycle nutrients and reduce the impact on phytoplankton NPP, as illustrated in the High Loss experiment (see Fig 3). A more diverse representation of phytoplankton functional types could also alter the magnitude and spatial pattern of NPP responses. This makes the simulated phytoplankton response in this study a first-order biogeochemical estimate of potential competition effects.

Sustaining large-scale global macroalgal cultivation required Fe supplementation, which drove a $\sim$90% increase in surface DFe and up to three times increase at the seafloor due to the remineralisation of biomass deposition. Despite the DFe enrichment phytoplankton NPP biomass declined by nearly half (see Fig. 3, Table 3) due to macronutrient robbing by macroalgae. An ocean Fe fertilisation modelling study also showed large-scale Fe fertilisation caused enhanced consumption of major nutrients in surface waters, and also reduces nutrients availability for lower latitudes, which offsets overall NPP (Tagliabue et al., 2023). This suggests that mCDR approaches can risk redistributing ecological pressure, while also suppressing additional carbon removal from phytoplankton.

Deep-sea biogeochemistry will also be altered due to macroalgal deposition. In the default simulation, deep-sea oxygen losses can reach suboxic levels in deposition zones (Fig. 5j-l) which has been a concern in previous studies (Wu et al., 2023; Levin et al., 2023; Chopin et al., 2024). Severe deoxygenation would favour smaller species, reduces large predators and bioturbation, and triggers faunal emergence or habitat avoidance, especially in the coastal benthos (Levin et al., 2023, 2009), which may alter natural carbon sequestration in the deep sea environment. Deposition also increases DIN at the seafloor (Table 3) and the introduction of nutrients to the oligotrophic seafloor may also alter benthic species interactions (Levin et al., 2023). We note that these results are not a detailed characterisation of benthic ecosystem impacts. MEDUSA's representation is intentionally simple, and a full assessment of seafloor community responses, including benthic respiration dynamics and faunal impacts, would require dedicated benthic ecological models. However, these results may be used to identify large-scale signals and pattens that would motivate future benthic studies.

4.2 Model Sensitivities

To examine how these impacts depend on cultivation and modelling design, we tested alternative harvesting threshold, extraction, loss rates, and nutrient limitations. Harvest timing and threshold can affect the optimal yield and capital expenditure (Bak et al., 2018). Lowering the harvest threshold improved CDR flux and efficiencies, both $CDR_{eff\ Harv}$ and $CDR_{eff\ NPP}$, while slightly reducing biogeochemical disruption, and with similar CDR flux as the default run. A field study has showed that a more frequent harvest without re-seeding, would increase yield per meter growth line and reduced cultivation cost (Bak et al., 2018, 2020). However, it also resulted in a greater decline in zooplankton biomass than phytoplankton biomass (Table 3) indicating potential downstream effects of macroalgae cultivation on higher trophic levels and, potentially, fisheries (Guibourd de Luzinais et al., 2023; Kwiatkowski et al., 2019). Higher thresholds allow more macroalgae biomass to accumulate ahead of harvesting, leading to an increase in macroalgal NPP. However, as more of this NPP is lost to non-harvesting losses in the model, the associated CDR efficiency is actually lower compared to other harvest experiments (Fig. 3). Further, by increasing the quantity of harvested material transferred to depth, higher thresholds additionally cause greater seafloor oxygen depletion, as well as a larger reduction in the NPP of phytoplankton (Table 3, Fig. 5k).

Other modelling and cultivation protocols can also significantly affect macroalgae production and CDR capacity. When non-harvesting loss is doubled, the macroalgae NPP is reduced by 2.20 Pg C yr^{-1} and its CDR flux, by 3.7 Pg C yr^{-1}, making it less efficient (Fig. 3a). High-loss experiments also lose less surface DIN compared to the default run because of higher remineralisation near the surface. In farmed macroalgae, non-harvesting loss due to falloff and frond erosion can reach more than 10% of its growth rate (Zhang et al., 2012). This simulation explores how CO_2 flux and ocean biogeochemistry are affected when non-harvesting loss consume more of macroalgal biomass. When harvested biomass is extracted rather than sunk to the deep ocean, CDR efficiencies become slightly higher than the default simulation because of the lack of carbon leaking when depositing macroalgae at shallower depths. This simulation also shows minimal impacts at the seafloor due to the absence of deposition (Table 3).

The CDR capacity of macroalgae is lower when Fe is not supplemented, since most areas of the open ocean will not be suitable for growing macroalgae (Paine et al., 2023). When Fe limitation is implemented, macroalgae NPP collapsed with

a 73.7% decrease in magnitude, aligning with recent work by Berger et al. (2025), and simulate a net increase in CO_2 flux to the atmosphere of 0.2 Pg C yr^{-1} . However, due to the positive bias in Fe concentration in MEDUSA, compared to the major decline of macroalgae harvest in the Southern Ocean that is simulated in Berger et al. (2025), the decline in this study is not as dramatic. The Fe limitation experiment also simulated 30.7% less DFe concentrations in surface waters than the control model (Table 3), further depressing phytoplankton NPP in the Southern Ocean, Equatorial Pacific, and subpolar North Atlantic. This simulation emphasises that large-scale macroalgal CDR depends critically on Fe supplementation and the enhanced CO_2 uptake simulated under Fe-replete conditions depends on nutrient subsidies.

4.3 Challenges for Implementation and Uncertainties

In carbon dioxide removal, additionality denotes that an mCDR strategy must demonstrate more CO_2 uptake relative to what would occur without it which will require model assessments due to the global scale of impacts and potential feedbacks between reservoirs (Bach et al., 2024). Assessing the additionality of macroalgae-based mCDR can be challenging because its CO_2 uptake enhancement is tightly coupled to the redistribution of nutrients and phytoplankton NPP loss within the ocean. In our simulation large-scale cultivation suppressed phytoplankton NPP both within and beyond cultivation areas (Fig. 6 & Supplementary figure S7), and this can complicate the measurement of net carbon removed (Bach et al., 2024). In terms of macroalgal cultivation, even with Fe supplementation, the increase of macroalgae biomass is at the expense of natural biological carbon export (Bach et al., 2021; Berger et al., 2023; Wu et al., 2023). According to the framework of Bach et al. (2024) macroalgae cultivation may show even smaller additionality since the carbon cost for setting up offshore macroalgae farm can be more than half of the potential CDR (Coleman et al., 2022).

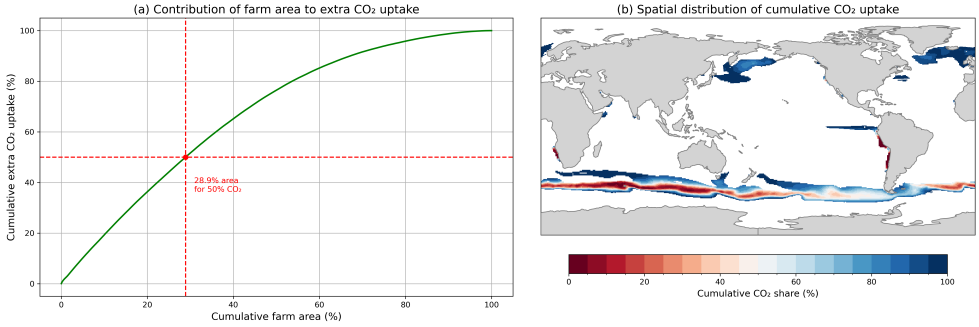

Figure 7. Large variation in CO_2 uptake within macroalgae cultivation areas. (a) Model grid cells are sorted by their quantitative contributions to additional CO_2 uptake and then the associated cultivation area and CO_2 uptake are accumulated. (b) Geographical distribution of cultivation area which contributes the most to additional CO_2. Deep red regions are those that contribute most to CO_2 uptake, while deep blue regions contribute least.

Compared to abiotic approaches, such as coastal ocean alkalinity enhancement (OAE), our large-scale macroalgal cultivation uptake is less spatially concentrated. Using the same modelling framework, Palmiéri and Yool (2024) reported that 13.8% of

the shelf accounts for 50% of the total extra CO_2 flux, with warmer areas contributing higher CO_2 uptake, indicating that CDR flux is dominated by a few high efficiency regions. In contrast, our default macroalgae simulation indicates that 28.9% of the cultivation area is required to reach the same proportion (Fig. 7a). The regions driving this uptake coincide with areas of high macroalgae NPP and CDR flux (Fig. 2b & Fig. 4b) particularly subpolar Southern Ocean and coast of Chile, as shown in Fig. 7b, reflecting a more widespread uptake pattern. This difference arises from the tight nutrient constrain in macroalgae-cultivation, while in OAE, additional CO_2 uptake is dependent on temperature, that enhances dissolution rate and the geography of the shelf. Furthermore, the rate of air-sea CO_2 gas transfer, parameterised following Wanninkhof (2014) as a function of local wind speed, introduces a natural lag between biological carbon drawdown and atmospheric CO2 uptake. DIC deficits that persist beyond a single growing season continue to drive CO2 uptake as surface waters are re-exposed to the atmosphere through seasonal mixed layer dynamics and circulation. This explains the regional variation in CDR efficiency shown in Figure 4c. In the Equatorial Pacific, relatively high macroalgal NPP is associated with lower CDR efficiency. In contrast, the deeper mixed layer in the Southern Ocean keeps low-DIC water in contact with the atmosphere for longer, resulting in higher efficiency. Although regions where high cumulative CO_2 share, CDR flux, and macroalgae NPP are located in the Southern Ocean, this area may not be suitable. Large-scale offshore macroalgae deployment would require extensive floating infrastructure, long-distance operations, and resilience to extreme wave and weather conditions (Jiao et al., 2025; Kwon et al., 2024). Such engineering and logistical considerations are not represented in the present model and remain outside the scope of this study.

Macroalgal extraction and product substitution can offer co-benefits such as substituting high-emission products with seaweed-based alternative. However, life-cycle analyses show that processing macroalgal products can offset much of the theoretical climate advantage (Jiao et al., 2025). A recent economic model estimates that product substitution yields a net profit of $\sim$US\$50 per tCO_2 avoided, compared to a cost of US\$480 per tCO_2 for deep-ocean deposition (DeAngelo et al., 2022), and product substitution could cut regional emissions by up to 13%, whereas direct sequestration contributes relatively little (Bullen et al., 2024). Together these studies highlight the importance of robust monitoring, reporting, and verification frameworks that can verify additionality and durable sequestration.

Natural climate solutions, such as saltmarshes, mangroves, and seagrass ecosystems or coastal macroalgal cultivation, can deliver both carbon sequestration and a range of co-benefits, including coastal protection, nutrient retention, and biodiversity support (Macreadie et al., 2021; Pessarrodona et al., 2023). These systems provide relatively direct and more verifiable carbon storage through sediment burial, while also helping mitigate eutrophication. Such coastal approaches may offer more tractable mCDR deployment, even though at smaller scale. These findings reinforce that no single approach is likely to deliver the required scale of carbon removal.

Several model limitations highlight the need for cautious interpretation of the quantitative estimates. Although MEDUSA captures the patterns and concentration of macronutrients fairly well (Yool et al., 2021), the model tends to overestimates DFe concentrations in regions known for persistent Fe limitation (Tagliabue et al., 2016). Additionally, our macroalgae module lacks variable stoichiometry (Arzeno-Soltero et al., 2023), DOC release (Paine et al., 2021), and explicit macroalgal grazing and erosion (Wu et al., 2023, 2025; Arzeno-Soltero et al., 2023). The model also does not represent calcifying epibionts that commonly colonise sargassum, and their calcification can offset CDR (Bach et al., 2021). Furthermore, MEDUSA does not

resolve coccolithophores phytoplankton types, meaning that potential reduction in calcite ballasting due to the reduction in phytoplankton concentration, are not captured. These omissions would act to further reduce CDR efficiency.

The absence of riverine nutrient inputs and coastal-shelf processes also prevents realistic simulation of Sargassum dynamics (Wang et al., 2019) and likely underestimates the productive potential of warm-water cultivation in regions such as Southeast and East Asia where terrestrial nutrient subsidies support high macroalgal biomass in nearshore systems. Although the four taxa represented in this study span a range of thermal niches, cold and warm water taxa are associated with different cultivation systems, whereby warm water species are usually farmed using single step methods through vegetative propagation and low-cost fixed or floating raft systems in nearshore environments (Behera et al., 2022) while cold water species require multi-step propagation from spores, hatchery-based seeding, and deployment on longlines system (Boderskov et al., 2023; Bak et al., 2020). These differences are not captured in this idealised framework and may mean that the modelled growth potential presented here translates differently to real-world aquaculture output depending on the region in question.

Although MEDUSA includes deoxygenation and acidification processes, the simplicity of its benthic ecosystem model cannot represent the impacts of such mechanisms on the seafloor ecosystems. While some processes may be partially represented within MEDUSA's remineralisation scheme, a targeted evaluation of acidification dynamics was beyond the scope of this study. Our results should be interpreted as a first order approximation of the biogeochemical consequences of large-scale macroalgae cultivation, and that representing these additional processes in future model developments will be important in estimating macroalgal CDR potential

Taken together, our results reinforce growing concerns that large-scale macroalgae cultivation may offer limited net climate benefits when ecological externalities and feedbacks are considered (Bach et al., 2021; Gallagher et al., 2022; Hurd et al., 2022). Despite its theoretical potential, macroalgal CDR appears constrained by nutrient bottlenecks, competition with natural carbon pumps, and low CDR capacity compared to macroalgal NPP. These findings point to the need for regionally tailored deployment, modelling and observation monitoring strategies, and explicit additionality accounting if macroalgal cultivation is to play a role in future climate mitigation portfolios.

5 Conclusions

This study provides a global-scale assessment of macroalgae cultivation within a coupled ocean biogeochemical model. Our simulations highlight the potential for carbon sequestration, while also revealing significant trade-offs, as well as sensitivities to model assumptions and different cultivation strategies. Given the uncertainties and model limitations, the results presented here should be interpreted as a first-order approximation of the biogeochemical consequences of large-scale macroalgae cultivation. Overall, our findings suggest that solely relying on large-scale macroalgae cultivation is unlikely to provide a viable mCDR solution, and that mitigation efforts will likely need to be distributed across different mCDR strategies, such as OAE and coastal ecosystem restoration. The key findings of this study are summarised as follows:

- This study presents a global scale implementation of a macroalgae cultivation module within a coupled OBGC model, and evaluates the carbon removal potential and biogeochemical impacts of this activity under multiple cultivation strategies and assumptions.

- We find that while macroalgae cultivation can enhance the net air–sea CO_2 flux into the ocean by up to 11.0 Pg C yr^{-1} when supplemented with Fe, the associated CDR efficiency is a modest 27.3% relative to the macroalgae productivity driving it.

- However, these fluxes come at the cost of substantial alterations to ocean biogeochemistry and ecosystems. In the default case, macroalgal growth reduces surface DIN concentrations by 53.1%, resulting in suppression of phytoplankton primary production by 49.8%, and global reductions in phytoplankton and zooplankton biomass, by 45.4% and 47.2%, respectively.

- When macroalgae are harvested and deposited, seafloor oxygen will decline globally by 20.3% and cause suboxic conditions in 7.9% of the seafloor, compared to 0.5% in the control model, especially within the deposition zones.

- The magnitude and spatial footprint of these impacts are strongly modulated by cultivation protocol, with more frequent harvesting improving CDR efficiency but intensifying the simulated oxygen depletion at depth caused by macroalgae biomass dumping.

- Exploration of other cultivation protocols and model assumptions, finds significant changes in macroalgae production and CO_2 flux. For example, Fe limitation of macroalgae growth actually causes outgassing by contributing 0.2 Pg C yr^{-1} to the atmosphere, indicating that scaled-up macroalgae cultivation without Fe fertilisation is not an effective mCDR technique.

Code availability. The FORTRAN code for macroalgae module and MEDUSA model can be found in: https://tinyurl.com/58wst8wj

Data availability. The model output that support the findings of this study will be openly available upon manuscript acceptance.

Author contributions. EKP, AY, and CAB acquired funding. PA, AY, and JP developed the macroalgae module. PA and AY conceptualised the study. PA performed the simulations, model output analysis, writing the first draft, and produced the figures. All authors contributed to ideas, participated in discussions of the results, and editing of the manuscript.

Competing interests. The authors declare that they have no conflict of interests.

Disclaimer. TEXT

Acknowledgements. The authors are grateful to the National Oceanography Centre's High-Performance Computing (HPC) system, which facilitated model simulation and analysis. All authors are funded by UK Research and Innovation (UKRI) under National Capability Science Multi-Centre (NCSMC) funding for Atlantic Climate and Environment Strategic Science (AtlantiS; NE/Y005589/1). Additionally, PA, AY, EP, and JP are funded under NCSMC funding for Future Impacts, Risks, and Mitigation Actions in a changing Earth system project (TerraFIRMA LTSM; NE/W004895/1). The Python code used to generate figures in this manuscript was written with the help of ChatGPT.

References

Aldridge, J., Mooney, K., Dabrowski, T., and Capuzzo, E.: Modelling effects of seaweed aquaculture on phytoplankton and mussel production. Application to Strangford Lough (Northern Ireland), Aquaculture, 536, 736 400, https://doi.org/10.1016/j.aquaculture.2021.736400, 2021.

Alevizos, E. and Barillé, L.: Global ocean spatial suitability for macroalgae offshore cultivation and sinking, Front. Mar. Sci., 10, 1320 642, https://doi.org/10.3389/fmars.2023.1320642, 2023.

Arzeno-Soltero, I. B., Saenz, B. T., Frieder, C. A., Long, M. C., DeAngelo, J., Davis, S. J., and Davis, K. A.: Large global variations in the carbon dioxide removal potential of seaweed farming due to biophysical constraints, Commun Earth Environ, 4, 185, https://doi.org/10.1038/s43247-023-00833-2, 2023.

Bach, L. T., Tamsitt, V., Gower, J., Hurd, C. L., Raven, J. A., and Boyd, P. W.: Testing the climate intervention potential of ocean afforestation using the Great Atlantic Sargassum Belt, Nat Commun, 12, 2556, https://doi.org/10.1038/s41467-021-22837-2, 2021.

Bach, L. T., Vaughan, N. E., Law, C. S., and Williamson, P.: Implementation of marine CO2 removal for climate mitigation: The challenges of additionality, predictability, and governability, Elem Sci Anth, 12, 00 034, https://doi.org/10.1525/elementa.2023.00034, 2024.

Bak, U. G., Mols-Mortensen, A., and Gregersen, O.: Production method and cost of commercial-scale offshore cultivation of kelp in the Faroe Islands using multiple partial harvesting, Algal Research, 33, 36–47, https://doi.org/https://doi.org/10.1016/j.algal.2018.05.001, 2018.

Bak, U. G., Gregersen, O., and Infante, J.: Technical challenges for offshore cultivation of kelp species: lessons learned and future directions, Botanica Marina, 63, 341–353, https://doi.org/10.1515/bot-2019-0005, 2020.

Barrett, L. T., Theuerkauf, S. J., Rose, J. M., Alleway, H. K., Bricker, S. B., Parker, M., Petrolia, D. R., and Jones, R. C.: Sustainable growth of non-fed aquaculture can generate valuable ecosystem benefits, Ecosystem Services, 53, 101 396, https://doi.org/https://doi.org/10.1016/j.ecoser.2021.101396, 2022.

Behera, D. P., Vadodariya, V., Veeragurunathan, V., Sigamani, S., Moovendhan, M., Srinivasan, R., Kolandhasamy, P., and Ingle, K. N.: Seaweeds cultivation methods and their role in climate mitigation and environmental cleanup, Total Environment Research Themes, 3-4, 100 016, https://doi.org/10.1016/j.totert.2022.100016, 2022.

Berger, M., Kwiatkowski, L., Ho, D. T., and Bopp, L.: Ocean dynamics and biological feedbacks limit the potential of macroalgae carbon dioxide removal, Environ. Res. Lett., 18, 024 039, https://doi.org/10.1088/1748-9326/acb06e, 2023.

Berger, M., Kwiatkowski, L., Bopp, L., and Ho, D. T.: Efficacy of seaweed-based carbon dioxide removal reduced by iron limitation and nutrient competition with phytoplankton, CDRxiv [Preprints], https://doi.org/https://doi.org/10.70212/cdrxiv.2025385.v1, preprint, 2025.

Boderskov, T., Rasmussen, M. B., and Bruhn, A.: Upscaling cultivation of Saccharina latissima on net or line systems; comparing biomass yields and nutrient extraction potentials, Front. Mar. Sci., 10, 992 179, https://doi.org/10.3389/fmars.2023.992179, 2023.

Boyd, P. and Vivian, C.M.G., e.: GESAMP “High level review of a wide range of proposed marine geoengineering techniques", Tech. rep., Joint Group of Experts on the Scientific Aspects of Marine Environmental Protection, 2019.

Boyd, P. W., Bach, L. T., Hurd, C. L., Paine, E., Raven, J. A., and Tamsitt, V.: Potential negative effects of ocean afforestation on offshore ecosystems, Nat Ecol Evol, 6, 675–683, https://doi.org/10.1038/s41559-022-01722-1, 2022.

Bullen, C. D., Driscoll, J., Burt, J., Stephens, T., Hessing-Lewis, M., and Gregr, E. J.: The potential climate benefits of seaweed farming in temperate waters, Sci Rep, 14, 15 021, https://doi.org/10.1038/s41598-024-65408-3, 2024.

Chen, J., Li, H., Zhang, Z., He, C., Shi, Q., Jiao, N., and Zhang, Y.: DOC dynamics and bacterial community succession during long-term degradation of Ulva prolifera and their implications for the legacy effect of green tides on refractory DOC pool in seawater, Water Research, 185, 116 268, https://doi.org/https://doi.org/10.1016/j.watres.2020.116268, 2020.

Choi, D., Lee, H.-G., Jung, Y.-H., Lee, D.-W., Han, J., Hyeon, J.-Y., and Choi, Y.-U.: Pilot-Scale Cultivation of Seaweed (Undaria pinnatifida) Along an Offshore Wind Farm in Southwestern Korea, Journal of Marine Science and Engineering, 13, https://doi.org/10.3390/jmse13050882, 2025.

Chopin, T., Costa-Pierce, B. A., Troell, M., Hurd, C. L., Costello, M. J., Backman, S., Buschmann, A. H., Cuhel, R., Duarte, C. M., Gröndahl, F., Heasman, K., Haroun, R. J., Johansen, J., Jueterbock, A., Lench, M., Lindell, S., Pavia, H., Ricart, A. M., Sundell, K. S., and Yarish, C.: Deep-ocean seaweed dumping for carbon sequestration: Questionable, risky, and not the best use of valuable biomass, One Earth, p. S2590332224000356, https://doi.org/10.1016/j.oneear.2024.01.013, 2024.

Chung, I. K., Beardall, J., Mehta, S., Sahoo, D., and Stojkovic, S.: Using marine macroalgae for carbon sequestration: a critical appraisal, Journal of Applied Phycology, 23, 877–886, https://doi.org/10.1007/s10811-010-9604-9, 2011.

Coleman, S., Dewhurst, T., Fredriksson, D. W., St. Gelais, A. T., Cole, K. L., MacNicoll, M., Laufer, E., and Brady, D. C.: Quantifying baseline costs and cataloging potential optimization strategies for kelp aquaculture carbon dioxide removal, Frontiers in Marine Science, Volume 9 - 2022, https://doi.org/10.3389/fmars.2022.966304, 2022.

Corrigan, S., Brown, A. R., Ashton, I. G. C., Smale, D. A., and Tyler, C. R.: Quantifying habitat provisioning at macroalgal cultivation sites, Reviews in Aquaculture, 14, 1671–1694, https://doi.org/https://doi.org/10.1111/raq.12669, 2022.

DeAngelo, J., Azevedo, I., Bistline, J., Clarke, L., Luderer, G., Byers, E., and Davis, S. J.: Energy systems in scenarios at net-zero CO2 emissions, Nat Commun, 12, 6096, https://doi.org/10.1038/s41467-021-26356-y, 2021.

DeAngelo, J., Saenz, B. T., Arzeno-Soltero, I. B., Frieder, C. A., Long, M. C., Hamman, J., Davis, K. A., and Davis, S. J.: Economic and biophysical limits to seaweed farming for climate change mitigation, Nat. Plants, 9, 45–57, https://doi.org/10.1038/s41477-022-01305-9, 2022.

Duarte, C. M., Wu, J., Xiao, X., Bruhn, A., and Krause-Jensen, D.: Can Seaweed Farming Play a Role in Climate Change Mitigation and Adaptation?, Front. Mar. Sci., 4, https://doi.org/10.3389/fmars.2017.00100, 2017.

Duarte, C. M., Bruhn, A., and Krause-Jensen, D.: A seaweed aquaculture imperative to meet global sustainability targets, Nat Sustain, 5, 185–193, https://doi.org/10.1038/s41893-021-00773-9, 2021.

Enríquez, S., Duarte, C. M., Sand-Jensen, K., and Nielsen, S. L.: Broad-scale comparison of photosynthetic rates across phototrophic organisms, Oecologia, 108, 197–206, https://doi.org/10.1007/BF00334642, 1996.

Froehlich, H. E., Afflerbach, J. C., Frazier, M., and Halpern, B. S.: Blue Growth Potential to Mitigate Climate Change through Seaweed Offsetting, Current Biology, 29, 3087–3093.e3, https://doi.org/10.1016/j.cub.2019.07.041, 2019.

Gallagher, J. B., Shelamoff, V., and Layton, C.: Seaweed ecosystems may not mitigate CO2 emissions, ICES Journal of Marine Science, 79, 585–592, https://doi.org/10.1093/icesjms/fsac011, 2022.

Group, N. S. I. W.: Sea Ice modelling Integrated Initiative (SI^3) – The NEMO sea ice engine, https://doi.org/10.5281/zenodo.7534900, 2023.

Guibourd de Luzinais, V., du Pontavice, H., Reygondeau, G., Barrier, N., Blanchard, J. L., Bornarel, V., Büchner, M., Cheung, W. W. L., Eddy, T. D., Everett, J. D., Guiet, J., Harrison, C. S., Maury, O., Novaglio, C., Petrik, C. M., Steenbeek, J., Tittensor, D. P., and Gascuel, D.: Trophic amplification: A model intercomparison of climate driven changes in marine food webs, PLOS ONE, 18, 1–23, https://doi.org/10.1371/journal.pone.0287570, 2023.

Hayashi, L., Reis, R. P., Dos Santos, A. A., Castelar, B., Robledo, D., De Vega, G. B., Msuya, F. E., Eswaran, K., Yasir, S. M., Ali, M. K. M., and Hurtado, A. Q.: The Cultivation of Kappaphycus and Eucheuma in Tropical and Sub-Tropical Waters, in: Tropical Seaweed Farming Trends, Problems and Opportunities, edited by Hurtado, A. Q., Critchley, A. T., and Neish, I. C., pp. 55–90, Springer International Publishing, Cham, ISBN 978-3-319-63497-5 978-3-319-63498-2, https://doi.org/10.1007/978-3-319-63498-2_4, 2017.

Hersbach, H., Bell, B., Berrisford, P., Hirahara, S., Horányi, A., Muñoz-Sabater, J., Nicolas, J., Peubey, C., Radu, R., Schepers, D., Simmons, A., Soci, C., Abdalla, S., Abellan, X., Balsamo, G., Bechtold, P., Biavati, G., Bidlot, J., Bonavita, M., De Chiara, G., Dahlgren, P., Dee, D., Diamantakis, M., Dragani, R., Flemming, J., Forbes, R., Fuentes, M., Geer, A., Haimberger, L., Healy, S., Hogan, R. J., Hólm, E., Janisková, M., Keeley, S., Laloyaux, P., Lopez, P., Lupu, C., Radnoti, G., de Rosnay, P., Rozum, I., Vamborg, F., Villaume, S., and Thépaut, J.-N.: The ERA5 global reanalysis, Quarterly Journal of the Royal Meteorological Society, 146, 1999–2049, https://doi.org/https://doi.org/10.1002/qj.3803, 2020.

Hurd, C. L., Harrison, P. J., Bischof, K., and Lobban, C. S.: Seaweed Ecology and Physiology, Cambridge University Press, Cambridge, 2014.

Hurd, C. L., Law, C. S., Bach, L. T., Britton, D., Hovenden, M., Paine, E. R., Raven, J. A., Tamsitt, V., and Boyd, P. W.: Forensic carbon accounting: Assessing the role of seaweeds for carbon sequestration, Journal of Phycology, 58, 347–363, https://doi.org/10.1111/jpy.13249, 2022.

Hurd, C. L., Gattuso, J., and Boyd, P. W.: Air-sea carbon dioxide equilibrium: Will it be possible to use seaweeds for carbon removal offsets?, Journal of Phycology, p. jpy.13405, https://doi.org/10.1111/jpy.13405, 2023.

Hwang, E. K., Liu, F., Lee, K. H., Ha, D. S., and Park, C. S.: Comparison of the cultivation performance between Korean (Sugwawon No. 301) and Chinese strains (Huangguan No. 1) of kelp Saccharina japonica in an aquaculture farm in Korea, Algae, 33, 101–108, https://doi.org/10.4490/algae.2018.33.2.4, 2018.

IPCC: Summary for Policymakers, p. 3–48, Cambridge University Press, 2022.

Jiang, Z., Fang, J., Mao, Y., Han, T., and Wang, G.: Influence of Seaweed Aquaculture on Marine Inorganic Carbon Dynamics and Sea-air < CO_2 Flux, J World Aquaculture Soc, 44, 133–140, https://doi.org/10.1111/jwas.12000, 2013.

Jiao, T., Feng, E. Y., Li, Y., and Tian, Y.: Carbon dioxide removal dilemma of macroalgae products: Evidence from carbon footprint and profitability, Journal of Cleaner Production, 492, 144 870, https://doi.org/10.1016/j.jclepro.2025.144870, 2025.

Jones, D. C., Ito, T., Takano, Y., and Hsu, W.-C.: Spatial and seasonal variability of the air-sea equilibration timescale of carbon dioxide, Global Biogeochemical Cycles, 28, 1163–1178, https://doi.org/https://doi.org/10.1002/2014GB004813, 2014.

Kennedy, J. R. and Blain, C. O.: A systematic review of marine macroalgal degradation: Toward a better understanding of macroalgal carbon sequestration potential, Journal of Phycology, 61, 399–432, https://doi.org/10.1111/jpy.70031, 2025.

Koesling, M., Kvadsheim, N. P., Halfdanarson, J., Emblemsvåg, J., and Rebours, C.: Environmental impacts of protein-production from farmed seaweed: Comparison of possible scenarios in Norway, Journal of Cleaner Production, 307, 127 301, https://doi.org/10.1016/j.jclepro.2021.127301, 2021.

Krause-Jensen, D. and Duarte, C. M.: Substantial role of macroalgae in marine carbon sequestration, Nature Geosci, 9, 737–742, https://doi.org/10.1038/ngeo2790, 2016.

Kwiatkowski, L., Aumont, O., and Bopp, L.: Consistent trophic amplification of marine biomass declines under climate change, Global Change Biology, 25, 218–229, https://doi.org/10.1111/gcb.14468, 2019.

Kwon, H., Hawkins, T. R., Zaimes, G. G., Infante, J., Kite-Powell, H. L., Stekoll, M. S., Roberson, L., Zotter, B., Augyte, S., Rocheleau, G., and Sims, N.: Life-cycle analysis of offshore macroalgae production systems in the United States, Algal Research, 82, 103 654, https://doi.org/https://doi.org/10.1016/j.algal.2024.103654, 2024.

Lauvset, S. K., Key, R. M., Olsen, A., van Heuven, S., Velo, A., Lin, X., Schirnick, C., Kozyr, A., Tanhua, T., Hoppema, M., Jutterström, S., Steinfeldt, R., Jeansson, E., Ishii, M., Perez, F. F., Suzuki, T., and Watelet, S.: A new global interior ocean mapped climatology: the $1^\circ \times 1^\circ$ GLODAP version 2, Earth System Science Data, 8, 325–340, https://doi.org/10.5194/essd-8-325-2016, 2016.

Levin, L. A., Ekau, W., Gooday, A. J., Jorissen, F., Middelburg, J. J., Naqvi, S. W. A., Neira, C., Rabalais, N. N., and Zhang, J.: Effects of natural and human-induced hypoxia on coastal benthos, Biogeosciences, 6, 2063–2098, https://doi.org/10.5194/bg-6-2063-2009, 2009.

Levin, L. A., Alfaro-Lucas, J. M., Colaço, A., Cordes, E. E., Craik, N., Danovaro, R., Hoving, H.-J., Ingels, J., Mestre, N. C., Seabrook, S., Thurber, A. R., Vivian, C., and Yasuhara, M.: Deep-sea impacts of climate interventions, Science, 379, 978–981, https://doi.org/10.1126/science.ade7521, 2023.

Macreadie, P. I., Costa, M. D. P., Atwood, T. B., Friess, D. A., Kelleway, J. J., Kennedy, H., Lovelock, C. E., Serrano, O., and Duarte, C. M.: Blue carbon as a natural climate solution, Nat Rev Earth Environ, 2, 826–839, https://doi.org/10.1038/s43017-021-00224-1, 2021.

Madec, G.: NEMO ocean engine, Tech. rep., Institut Pierre-Simon Laplace No 27, https://doi.org/ISSN No 1288-1619., publication Title: Note du Pole de modelisation Issue: 27, 2016.

Magcanta-Mortos, M. L. M., Tahiluddin, A. B., Mortos, J. M. R., Aspe, N. M., Aaron-Amper, J., Leopardas, V. E., and Uy, W. H.: Sargassum hatchery-based cultivation and mariculture techniques in the Philippines: Practices, challenges, and future prospects, Aquatic Botany, 201, 103 925, https://doi.org/10.1016/j.aquabot.2025.103925, 2025.

Naylor, R. L., Hardy, R. W., Buschmann, A. H., Bush, S. R., Cao, L., Klinger, D. H., Little, D. C., Lubchenco, J., Shumway, S. E., and Troell, M.: A 20-year retrospective review of global aquaculture, Nature, 591, 551–563, https://doi.org/10.1038/s41586-021-03308-6, 2021.

N'Yeurt, A. D. R., Chynoweth, D. P., Capron, M. E., Stewart, J. R., and Hasan, M. A.: Negative carbon via Ocean Afforestation, Process Safety and Environmental Protection, 90, 467–474, https://doi.org/10.1016/j.psep.2012.10.008, 2012.

Ocean Visions and Monterey Bay Aquarium Research Institute: Answering Critical Questions About Sinking Macroalgae for Carbon Dioxide Removal: A Research Framework to Investigate Sequestration Efficacy and Environmental Impacts, Tech. rep., Ocean Visions; Monterey Bay Aquarium Research Institute, https://oceanvisions.org/wp-content/uploads/2022/10/Ocean-Visions-Sinking-Seaweed-Report_FINAL.pdf, available online, 2022.

Orr, J. C. and Epitalon, J.-M.: Improved routines to model the ocean carbonate system: mocsy 2.0, Geoscientific Model Development, 8, 485–499, https://doi.org/10.5194/gmd-8-485-2015, 2015.

Paine, E. R., Schmid, M., Boyd, P. W., Diaz-Pulido, G., and Hurd, C. L.: Rate and fate of dissolved organic carbon release by seaweeds: A missing link in the coastal ocean carbon cycle, Journal of Phycology, 57, 1375–1391, https://doi.org/https://doi.org/10.1111/jpy.13198, 2021.

Paine, E. R., Boyd, P. W., Strzepek, R. F., Ellwood, M., Brewer, E. A., Diaz-Pulido, G., Schmid, M., and Hurd, C. L.: Iron limitation of kelp growth may prevent ocean afforestation, Commun Biol, 6, 607, https://doi.org/10.1038/s42003-023-04962-4, 2023.

Palmiéri, J. and Yool, A.: Global-Scale Evaluation of Coastal Ocean Alkalinity Enhancement in a Fully Coupled Earth System Model, Earth's Future, 12, e2023EF004 018, https://doi.org/10.1029/2023EF004018, 2024.

Pessarrodona, A., Franco-Santos, R. M., Wright, L. S., Vanderklift, M. A., Howard, J., Pidgeon, E., Wernberg, T., and Filbee-Dexter, K.: Carbon sequestration and climate change mitigation using macroalgae: a state of knowledge review, Biological Reviews, 98, 1945–1971, https://doi.org/10.1111/brv.12990, 2023.

Peteiro, C., Sánchez, N., Dueñas-Liaño, C., and Martínez, B.: Open-sea cultivation by transplanting young fronds of the kelp Saccharina latissima, J Appl Phycol, 26, 519–528, https://doi.org/10.1007/s10811-013-0096-2, 2014.

Reagan, J. R., Boyer, T. P., García, H. E., Locarnini, R. A., Baranova, O. K., Bouchard, C., Cross, S. L., Mishonov, A. V., Paver, C. R., Seidov, D., Wang, Z., and Dukhovskoy, D.: World Ocean Atlas 2023, https://doi.org/10.25921/va26-hv25, dataset: NCEI Accession 0270533, 2024.

Roberts, D. A., Paul, N. A., Dworjanyn, S. A., Bird, M. I., and De Nys, R.: Biochar from commercially cultivated seaweed for soil amelioration, Sci Rep, 5, 9665, https://doi.org/10.1038/srep09665, 2015.

Roque, B. M., Salwen, J. K., Kinley, R., and Kebreab, E.: Inclusion of Asparagopsis armata in lactating dairy cows' diet reduces enteric methane emission by over 50 percent, Journal of Cleaner Production, 234, 132–138, 2019.

Ross, F., Tarbuck, P., and Macreadie, P. I.: Seaweed afforestation at large-scales exclusively for carbon sequestration: Critical assessment of risks, viability and the state of knowledge, Front. Mar. Sci., 9, 1015 612, https://doi.org/10.3389/fmars.2022.1015612, 2022.

Sato, Y., Fujiwara, T., and Endo, H.: Density regulation of aquaculture production and its effects on commercial profit and quality as food in the cosmopolitan edible seaweed Undaria pinnatifida, Frontiers in Marine Science, Volume 10 - 2023, https://doi.org/10.3389/fmars.2023.1085054, 2023.

Sato, Y., Saito, D., Inomata, E., Tanaka, A., and Nishihara, G. N.: Carbon and nitrogen contents depends on macroalgal species, their tissue section, and development stage, Phycological Research, https://doi.org/10.1111/pre.70007, 2025.

Sharma, S., Neves, L., Funderud, J., Mydland, L. T., Øverland, M., and Horn, S. J.: Seasonal and depth variations in the chemical composition of cultivated Saccharina latissima, Algal Research, 32, 107–112, https://doi.org/10.1016/j.algal.2018.03.012, 2018.

Sheppard, E. J., Hurd, C. L., Britton, D. D., Reed, D. C., and Bach, L. T.: Seaweed biogeochemistry: Global assessment of C:N and C:P ratios and implications for ocean afforestation, Journal of Phycology, 59, 879–892, https://doi.org/10.1111/jpy.13381, 2023.

Tagliabue, A., Aumont, O., DeAth, R., Dunne, J. P., Dutkiewicz, S., Galbraith, E., Misumi, K., Moore, J. K., Ridgwell, A., Sherman, E., Stock, C., Vichi, M., Völker, C., and Yool, A.: How well do global ocean biogeochemistry models simulate dissolved iron distributions?, Global Biogeochemical Cycles, 30, 149–174, https://doi.org/10.1002/2015GB005289, 2016.

Tagliabue, A., Twining, B. S., Barrier, N., Maury, O., Berger, M., and Bopp, L.: Ocean iron fertilization may amplify climate change pressures on marine animal biomass for limited climate benefit, Global Change Biology, 29, 5250–5260, https://doi.org/10.1111/gcb.16854, 2023.

Tullberg, R. M., Nguyen, H. P., and Wang, C. M.: Review of the Status and Developments in Seaweed Farming Infrastructure, Journal of Marine Science and Engineering, 10, https://doi.org/10.3390/jmse10101447, 2022.

Valderrama, D., Cai, J., Hishamunda, N., and Ridler, N.: Social and economic dimensions of carrageenan seaweed farming, Fisheries and aquaculture technical paper no. 580, Food and Agriculture Organization of the United Nations (FAO), Rome, Italy, ISBN 978-92-5-107746-7 (print); E-ISBN 978-92-5-107747-4 (PDF), https://www.fao.org/4/i3344e/i3344e.pdf, 2013.

Van Der Molen, J., Ruardij, P., Mooney, K., Kerrison, P., O'Connor, N. E., Gorman, E., Timmermans, K., Wright, S., Kelly, M., Hughes, A. D., and Capuzzo, E.: Modelling potential production of macroalgae farms in UK and Dutch coastal waters, Biogeosciences, 15, 1123–1147, https://doi.org/10.5194/bg-15-1123-2018, 2018.

Veenhof, R. J., Burrows, M. T., Hughes, A. D., Michalek, K., Ross, M. E., Thomson, A. I., Fedenko, J., and Stanley, M. S.: Sustainable seaweed aquaculture and climate change in the North Atlantic: challenges and opportunities, Frontiers in Marine Science, 11, 1483 330, https://doi.org/10.3389/fmars.2024.1483330, 2024.

Wang, M., Hu, C., Barnes, B. B., Mitchum, G., Lapointe, B., and Montoya, J. P.: The great Atlantic Sargassum belt, Science, 365, 83–87, https://doi.org/10.1126/science.aaw7912, 2019.

Wang, X., He, L., Ma, Y., Huan, L., Wang, Y., Xia, B., and Wang, G.: Economically important red algae resources along the Chinese coast: History, status, and prospects for their utilization, Algal Research, 46, 101 817, https://doi.org/https://doi.org/10.1016/j.algal.2020.101817, 2020.

Wanninkhof, R.: Relationship between wind speed and gas exchange over the ocean revisited, Limnology & Ocean Methods, 12, 351–362, https://doi.org/10.4319/lom.2014.12.351, 2014.

Wu, J., Keller, D. P., and Oschlies, A.: Carbon dioxide removal via macroalgae open-ocean mariculture and sinking: an Earth system modeling study, Earth Syst. Dynam., 14, 185–221, https://doi.org/10.5194/esd-14-185-2023, 2023.

Wu, J., Yao, W., Keller, D. P., and Oschlies, A.: Nearshore Macroalgae Cultivation for Carbon Sequestration by Biomass Harvesting: Evaluating Potential and Impacts With an Earth System Model, Geophysical Research Letters, 52, e2025GL116 774, https://doi.org/10.1029/2025GL116774, 2025.

Yamamoto, M., Kato, T., Kanayama, S., Nakase, K., and Tsutsumi, N.: Effectiveness of Iron Fertilization for Seaweed Bed Restoration in Coastal Areas, J. of Wat. & Envir. Tech., 15, 186–197, https://doi.org/10.2965/jwet.16-080, 2017.

Yool, A., Popova, E. E., and Anderson, T. R.: MEDUSA-2.0: an intermediate complexity biogeochemical model of the marine carbon cycle for climate change and ocean acidification studies, Geoscientific Model Development, 6, 1767–1811, https://doi.org/10.5194/gmd-6-1767-2013, iSBN: 1991-9603, 2013.

Yool, A., Palmiéri, J., Jones, C. G., de Mora, L., Kuhlbrodt, T., Popova, E. E., Nurser, A. J. G., Hirschi, J., Blaker, A. T., Coward, A. C., Blockley, E. W., and Sellar, A. A.: Evaluating the physical and biogeochemical state of the global ocean component of UKESM1 in CMIP6 historical simulations, Geoscientific Model Development, 14, 3437–3472, https://doi.org/10.5194/gmd-14-3437-2021, 2021.

Zhang, J., Fang, J., Wang, W., et al.: Growth and loss of mariculture kelp *Saccharina japonica* in Sungo Bay, China, Journal of Applied Phycology, 24, 1209–1216, https://doi.org/10.1007/s10811-011-9762-4, 2012.

Zhang, J., Wu, W., Ren, J. S., and Lin, F.: A model for the growth of mariculture kelp *Saccharina japonica* in Sanggou Bay, China, Aquaculture Environment Interactions, 8, 273–283, https://doi.org/10.3354/aei00171, 2016.

Zollmann, M., Liberzon, A., Palatnik, R. R., et al.: Effects of season, depth and pre-cultivation fertilizing on Ulva growth dynamics offshore the Eastern Mediterranean Sea, Scientific Reports, 13, 14 784, https://doi.org/10.1038/s41598-023-41605-4, 2023.